문서번호 APCC-출장-17-0563(2017-05-22)

TRAVEL REPORT FORM
출장보고서

결재	연구원	팀장	부서장	원장
	05/22 이현주	05/22 이우섭	05/22 유진호	05/22 정홍상
협조				

I. Reporter 보고자

Department 소속	Position 직위(직급)	Name 성명	Travel Date 날짜	Note 비고
기후예측본부 기후예측팀	선임연구원	손수진	2016/05/02~13	
기후예측본부 기후예측팀	연구원	이현주	2016/05/02~13	
기후예측본부 기후예측팀	연구원	김가영	2016/05/02~13	

II. Major Activities 주요업무 수행내용

1. Main Contents and Activities 주요내용 및 활동

가. 개요

○ 학회명 : 7th International Verification Methods Workshop의 tutorial 및 science conference(7IVMW)

- 7IVMW는 WMO Joint Working Group on Forecast Verification Research(JWGFVR)에서 주관하는 워크숍으로 기후예측 및 조기경보 시스템 등 다양한 시간/공간 규모의 예측 기술 검증 방법에 대한 토의/활용 및 그 진흥을 목적으로 개최됨.
- 7IVMW는 예측 검증 방법에 대한 강의와 R프로그램에 대한 hands-on으로 구성된 Tutorial Session과 예측 검증에 대한 연구 결과를 공유하는 Science Session으로 구성됨.
- 전세계 35개국의 예측현업 기관 및 학교, 연구기관에서 약 150명의 예측 검증 전문가가 참여하였으며, 80여편의 발표가 진행됨

○ 일시 : 2017년 5월 02일-13일

○ 장소 : (Tutorial Session) Max-Planck-Institute for Human Development(MPIB)
(Conference Session) VKU Forum in Berlin, Germany

나. 주요 업무 수행 사항

○ Tutorial Session

(1일차 교육 내용)

- Introduction to R
- Verification basics

- Data preparations
- Verification of forecast of continuous variables

(2일차 교육 내용)
- Verification of categorical forecast
- Probability and ensemble verification I
- Probability and ensemble verification II
- Verification of seasonal and subseasonal forecasts

(3일차 교육 내용)
- Statistical Inference
- Spatial forecast verification
- Operational verification systems
- Special Topics I : Multivariate Verifications

(4일차 교육 내용)
- Special Topics II : Assessing Value of forecasts
- Special Topics III : Observational uncertainty
- Special Topics IV : Warnings and extremes
- Special Topics V : Verification of non-standard variables

○ Conference Session : 발표 내용

발표자	발표세션	발표 제목
손수진	P S2S-2	Verification for long-lead station-scale prediction of hydrological droughts in South Korea based on bivariate pattern-based downscaling
이현주	P S2S-1	Evaluation of Heat Wave forecasting using large scale circulation pattern based on TIGGE data
김가영	P S2S-6	Assessment of WMO LC-LRFMME Models in Seasonal Climate Prediction
Team Project	Tutorial projcet presentation	Verification of deterministic precipitation forecasts

(사진 1) Tutorial Session 참가자

(사진 2) Team Project 참여 현장

2. Relevance to APEC Climate Center's Activities 결론 및 소감

○ 본 워크숍의 Tutorial Session을 통해 현재 센터에서 계절예측 검증 방법에 사용되는 기본적인 지식을 정리하고, 다양한 시·공간 규모의 예측 검증방법에 대한 지식을 습득하였으며, R 프로그램의 Hands-on을 통해 R프로그램에 대한 기본적인 사용 방법을 습득하여 당 센터의 연구 및 시스템 개발에 적극 활용 가능할 것으로 생각됨.

○ 본 워크숍의 Conference Session을 통해 현재 전세계적으로 관측자료의 불확실성에 대한 검증과 예측자료의 공간검증에 대한 관심이 높은 것을 확인 할 수 있었음.

○ 또한, 예측측면에서의 검증 뿐만 아니라 예측 자료의 후처리를 통한 응용연구/사용자 그룹에 적용된 최종 사용자 중심의 검증에 대한 연구도 활발히 진행중인 것이 확인됨에 따라 예측 자료의 최종 사용자와의 원활한 소통을 통해 보다 활용도 높은 예측 자료 생산 및 검증 또한 중요할 것으로 보임.

○ 그러나 당 센터에서 추진하고자 하는 S2S 연구의 검증 방법에 대한 연구는 미비한 것으로 판단되며, S2S 예측 연구와 더불어 검증 방법에 대한 연구를 추가적으로 수행해 나간다면 S2S 예측 연구 분야의 선도적인 역할을 할 수 있을 것으로 보임에 따라 이에 대한 지속적인 관심과 노력 필요함.

III. References 참고사항

(with attachment of any information or report in case of attendance of conferences, workshops and meetings) 학술대회, 워크숍, 회의 등 참석 시 관련 정보 및 문서 첨부

1. Presented and Collected Materials 주요 수집자료

    [붙임1]_7IVMW_Tutorial_Materials.zip
    [붙임2]_7IVMW_Presentations.zip

2. Suggestions and Remarks 건의사항

7th International Verification Methods Workshop
Tutorial Course 3-6 May 2017

Max Planck Institute
Berlin, Germany

Day 1 – Wednesday May 3

Time	Topic	Lead	Contents
09:00 – 09:10	Welcome	Dr. Ralph Hertwig, Director, MPI	Welcome message
09:10 – 09:30	Introductions	Laurie Wilson and Martin Göber	Housekeeping, trainers and tutorial students introduce themselves
09:30 – 11:00	Introduction to R	Sabrina Wahl, Philipp Zschenderlein	Brief introduction to R and a series of exercises focused on data manipulation and verification tools
11:00 – 11:30	Break		
11:30 – 13:00	Verification basics	Barb Brown	Basic statistics review; joint distribution of forecasts and observations; graphical methods for displaying the joint distribution and verification results
13:00 – 14:00	Lunch		
14:00 – 15:00	Data Preparation	C. Marsigli, L. Wilson	Principles guiding the compilation of datasets for verification; matching forecast and observation
15:00 – 15:30	Break		
15:30 – 17:00	Verification of forecasts of continuous variables	M. Dorninger	Scatter plots, bias, MAE, RMSE, correlation, reduction of variance; skill scores for continuous variables
17:00 – 17:30	Introduction to projects	L. Wilson	Projects will be assigned in advance using datasets obtained from participants. All projects will be supported by a clear list of instructions.
17:30 -	Icebreaker		

Day 2 – Thursday May 4

Time	Topic	Lead	Contents
09:00 – 10:30	Verification of categorical forecasts	L. Wilson	Why categorize? – contingency tables and scores with interpretation
10:30 – 11:00	Break		
11:00 – 13:00	Probability and ensemble verification I	C. Marsigli, C. Coelho	Probability definition; concepts of reliability; resolution; base rate; sharpness; scores; verification methods for EPS output
13:00 – 14:00	Lunch		
14:00 – 15:00	Probability and ensemble verification II	C. Coelho, C. Marsigli	Methods for measuring discrimination: The ROC
15:00 – 15:30	Break		

15:30 – 16:15	Verification of seasonal and subseasonal forecasts	C. Coelho	Verification methods applicable to longer range forecasts
16:15 – 18:00	Project time		Instructors available

Day 3 – Friday, May 5

Time	Topic	Lead	Contents
09:00 – 10:30	Statistical Inference	B. Brown	Confidence interval estimation – traditional and bootstrap methods; block bootstrap; inference
10:30 – 11:00	Break		
11:00 – 13:00	Spatial forecast verification	M. Dorninger, P. Zschenderlein	Why spatial verification; four types of methods; survey of methods with suggestions on their use and illustrative examples
13:00 – 14:00	Lunch		
14:00 – 15:00	Operational verification systems	M. Mittermaier	Illustrative examples of existing operational verification systems and how to set them up
15:00 – 15:30	Break		
15:30 – 16:30	Special Topics 1: Multivariate Verification	Prof. Andreas Hense	Verification metrics with more than one dimension: Purpose and examples.
16:30 – 18:00	Project Time		Instructors available

Day 4 – Saturday, May 6

Time	Topic	Lead	Contents
09:00 – 10:00	Special topics II: Assessing Value of forecasts	Jeff Lazo	Definition of value; introduction to the cost-loss model, with example(s)
10:00 – 10:30	Special Topics III: Observational uncertainty	B. Brown	Sources of uncertainty in observational data; estimation of observation errors.
10:30 – 11:00	Break		
11:00 – 11:45	Special topics IV: Warnings and extremes	M. Göber,	Verification of weather warnings and extremes
11:45 – 12:30	Special topics V: Verification of non-standard variables	B. Brown	Tropical cyclone verification, verification of non-meteorological variables such as sea ice motion and forest fires.
12:30 – 13:00	Wrap up	All	Any questions that have arisen during the tutorial – further discussion as needed.
13:00 – 14:00	Lunch		
14:00 – 17:30	Project time		

Assessment of WMO LC-LRFMME Models in Seasonal Climate Prediction

Gayoung Kim[1*], Joong-Bae Ahn[2], Vladimir N. Kryjov[3], Soo-Jin Sohn[1], Richard Graham[4], Rupa Kumar Kolli[5]

[1]APEC Climate Center, Busan, South Korea
[2]Pusan National University, Busan South Korea
[3]Hydrometeorological Research Center, Moscow, Russia
[4]Met Office Hadley Center, Exeter, UK
[5]World Meteorological organization, Geneva, Switzerland

Introduction

- Over the last two decades, dynamic climate models have undergone steady and diverse developments, and many international climate centres now exploit them to produce operational seasonal predictions. Despite these advances, prediction skill based on the models remains limited (e.g. Hagedorn *et al.*, 2005;Wang *et al.*, 2009).
- The multi-model ensemble (MME) method has been implemented and exploited by several major operational centres for seasonal prediction to overcome these problems and improving of prediction skill is the ensemble approach, in which forecasts from different prediction systems are combined.
- WMO LC-LRFMME, which is designated by WMO, issues 1-month lead seasonal predictions in both deterministic and probabilistic forms.
- In this study, we assess the MME-based forecast skill of WMO-designated global producing centres (GPCs) with a focus on regional climate outlook forum (RCOF) regions, because seasonal predictions from the Lead Centre are used by developing countries for their economic needs.

Models and observation datasets

- Models (GPCs): 1-month lead 3-month prediction for MAM, JJA, SON and DJF
- Observation
  - T2M: NCEP/NCAR reanalysis / PREC: CAMS OPI

Table 1. WMO Global Producing Centres (GPCs) with summary information of the forecast system configurations. More details are available at WMO LC-LRFMME website (www.wmolc.org).

GPC name (model)	Centre	Resolution (Atmospheric component)	Hindcast period used	System configuration (Ensemble size of hindcast)
Melbourne (POAMA M2.4)	Australian Bureau of Meteorology	T47/L17	1960-2010	Coupled (10)
Montreal (MSC CANCM3 & MSC CANCM4)	Meteorological Service of Canada	T63	1981-2010	Coupled (10)
Moscow (HMC)	Hydrometeorological Centre of Russia	1.125ºx 1.40625º /L28	1981-2010	2-tier (10)
Seoul (GDAPS)	Korea Meteorology Administration	T106/L21	1979-2012	2-tier (20)
Tokyo (JMA)	Japan Meteorological Agency	1.875º x1.875º /L40	1979-2010	Coupled (10)

Assessment of Prediction Skill over Globe

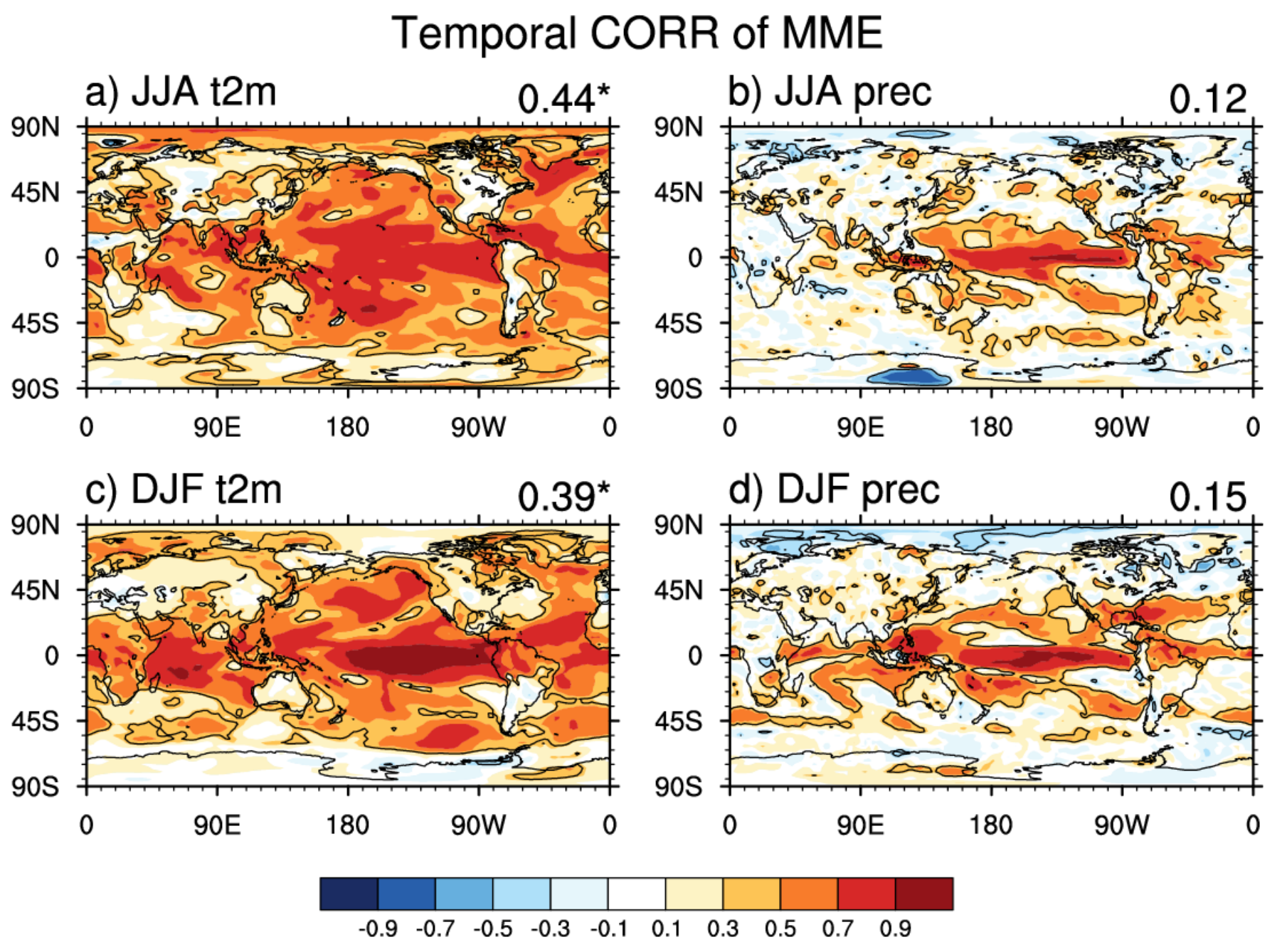

Fig. 1. Temporal correlation coefficient (TCC) of MME of (a) 2m temperature for JJA, (b) precipitation for JJA, (c) 2m temperature for DJF and (d) precipitation for DJF. The number on the upper right side of each plot represents the areal mean of global TCC. * and ** indicate 90% and 95% confidence levels, respectively. The contour lines indicate that the estimate score is significant at the 95% confidence level using the one-tailed Student's t test.

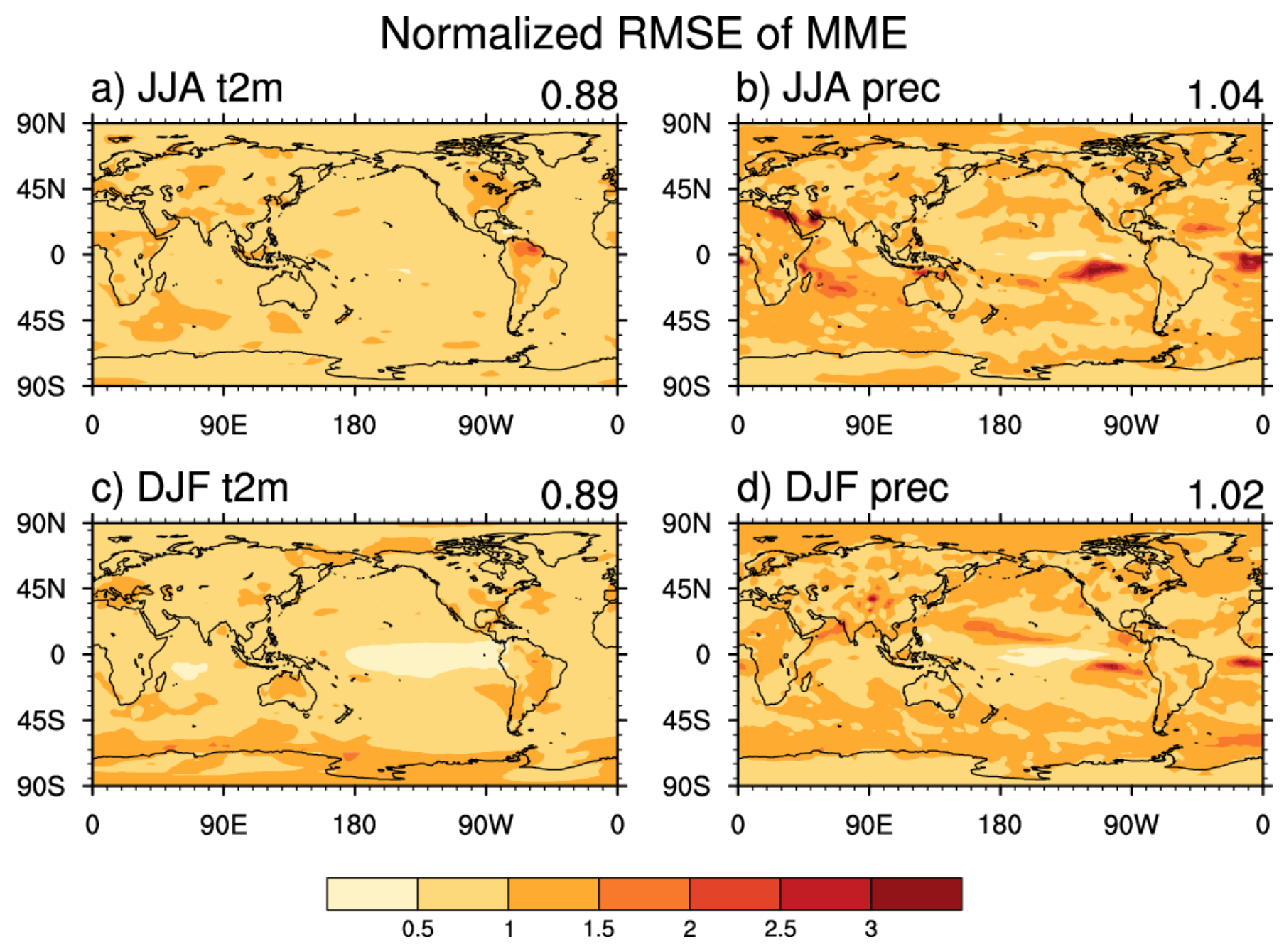

Fig. 2. Normalized root mean squared error (NRMSE) of MME of (a) 2m temperature for JJA, (b) precipitation for JJA, (c) 2m temperature for DJF and (d) precipitation for DJF. The number on the upper right side of each plot represents the areal mean of global NRMSE.

- The forecast skills (TCCs) and errors (NRMSEs) for 2m temperature are better than those of precipitation in both seasons.
- The seasonal variations of both variables for TCCs and NRMEs. Spatially, TCCs (NRMSEs) of 2m temperature over land are lower (higher) than those over the ocean for both seasons.

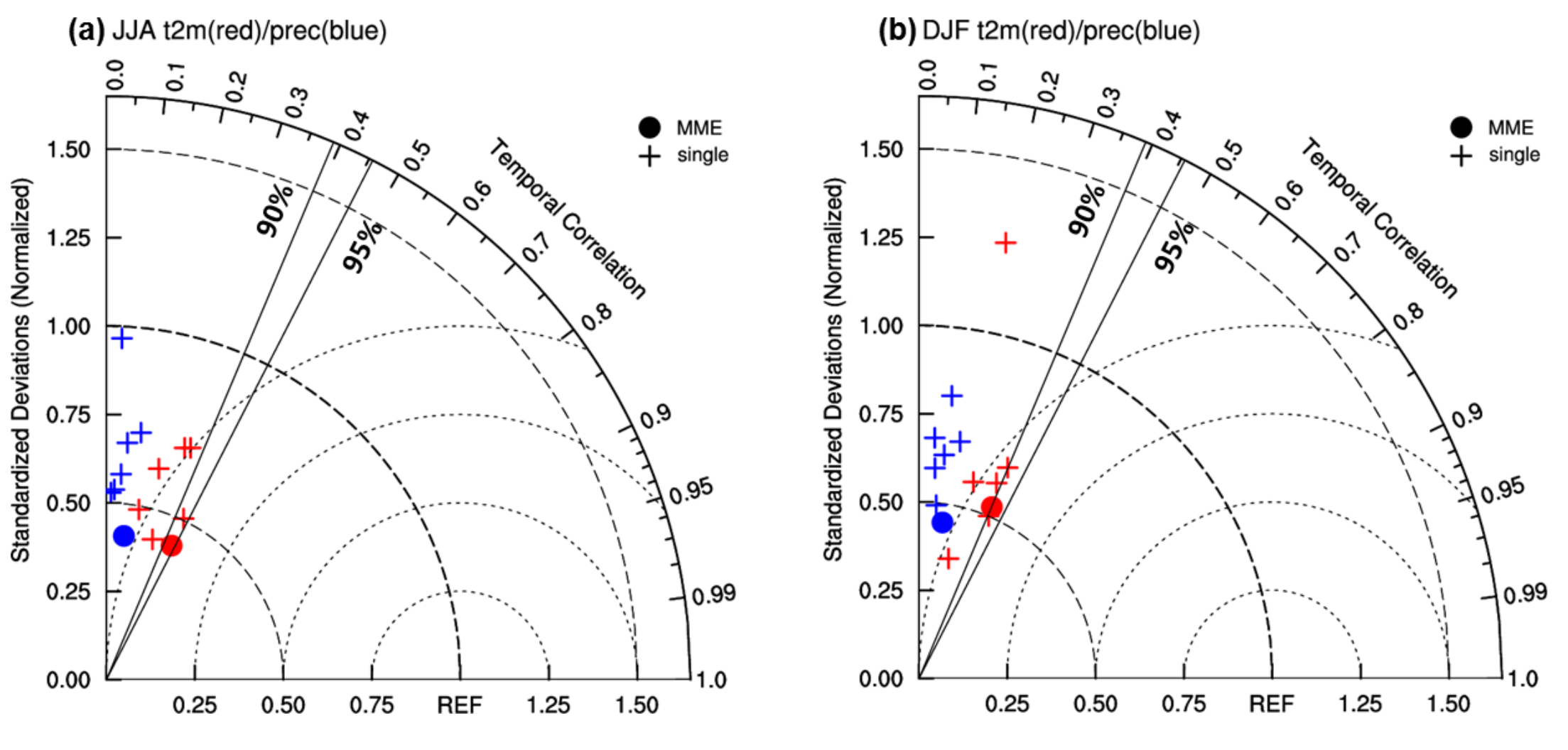

Fig. 3. Taylor diagrams between temporal correlation and normalized standard deviation of 2m temperature (red) and precipitation (blue) for (a) JJA and (b) DJF. The dots and crosses indicate MME and single models, respectively.

- The single models for the JJA temperature and precipitation show lower variability than the observed values.
- Some models can reproduce a similar variability as the observed values. However, the MME method reduces the individual models' variability, which is one of the limitations of the MME. The MME for the DJF season shows similar skill as JJA, whereas the variability of single models for temperature differed greatly from those of precipitation.

Assessment of Prediction Skill over 13 RCOF regions

Table 2. TCC of 2m temperature for MAM, JJA, SON and DJF over 13 RCOF regions for each single model and MME. Shading indicate 95% level of confidence, respectively.

		Model 1	Model 2	Model 3	Model 4	Model 5	Model 6	MEAN	MME
a) GHACOF	MAM	0.52	0.40	0.47	0.46	0.45	0.49	0.48	0.55
	JJA	0.30	0.24	0.23	0.34	0.34	0.39	0.32	0.40
	SON	0.41	0.27	0.35	0.47	0.44	0.41	0.41	0.50
	DJF	0.48	0.38	0.48	0.53	0.38	0.52	0.48	0.59
b) SARCOF	MAM	0.45	0.36	0.38	0.43	0.36	0.53	0.43	0.51
	JJA	0.26	0.25	0.19	0.22	0.26	0.36	0.27	0.34
	SON	0.32	0.33	0.28	0.35	0.30	0.35	0.33	0.40
	DJF	0.37	0.26	0.42	0.45	0.33	0.50	0.41	0.51
c) PRESAO	MAM	0.53	0.51	0.61	0.63	0.54	0.65	0.59	0.67
	JJA	0.51	0.39	0.31	0.37	0.51	0.65	0.48	0.60
	SON	0.56	0.49	0.56	0.58	0.53	0.65	0.57	0.63
	DJF	0.52	0.46	0.55	0.60	0.43	0.67	0.55	0.64
d) FOCRAII	MAM	0.44	0.37	0.47	0.52	0.41	0.56	0.47	0.56
	JJA	0.33	0.26	0.27	0.32	0.40	0.46	0.36	0.46
	SON	0.39	0.38	0.43	0.44	0.44	0.51	0.44	0.52
	DJF	0.34	0.26	0.41	0.44	0.34	0.51	0.40	0.51
e) WCSACOF	MAM	0.24	0.32	0.34	0.39	0.25	0.41	0.33	0.40
	JJA	0.28	0.27	0.21	0.18	0.25	0.43	0.28	0.34
	SON	0.26	0.27	0.29	0.27	0.28	0.31	0.29	0.35
	DJF	0.19	0.28	0.44	0.39	0.23	0.46	0.34	0.40
f) SSACOF	MAM	0.05	0.11	0.14	0.14	0.06	0.19	0.12	0.16
	JJA	0.08	0.20	0.16	0.13	0.09	0.35	0.18	0.28
	SON	-0.03	0.16	0.09	0.12	0.11	0.18	0.12	0.18
	DJF	-0.01	0.07	0.18	0.10	0.03	0.16	0.09	0.12
g) PICOF	MAM	0.59	0.55	0.61	0.65	0.64	0.70	0.64	0.72
	JJA	0.56	0.56	0.42	0.45	0.65	0.70	0.58	0.69
	SON	0.62	0.53	0.68	0.62	0.67	0.69	0.64	0.70
	DJF	0.51	0.47	0.56	0.60	0.59	0.66	0.58	0.65
h) CACOF	MAM	0.61	0.64	0.61	0.72	0.59	0.69	0.66	0.72
	JJA	0.63	0.49	0.44	0.56	0.56	0.76	0.59	0.72
	SON	0.60	0.50	0.70	0.70	0.62	0.74	0.66	0.75
	DJF	0.55	0.48	0.63	0.69	0.54	0.70	0.61	0.68
i) SEECOF	MAM	0.26	0.32	0.39	0.41	0.21	0.45	0.36	0.48
	JJA	0.32	0.11	0.12	0.16	0.42	0.24	0.24	0.35
	SON	0.12	0.20	0.20	0.21	0.01	0.17	0.16	0.21
	DJF	0.18	0.00	0.00	0.11	-0.15	0.21	0.05	0.01
j) SASCOF	MAM	0.39	0.42	0.48	0.51	0.46	0.55	0.49	0.60
	JJA	0.32	0.31	0.34	0.38	0.38	0.47	0.38	0.47
	SON	0.35	0.35	0.44	0.37	0.42	0.55	0.43	0.50
	DJF	0.37	0.32	0.43	0.39	0.35	0.48	0.41	0.51
k) CARICOF	MAM	0.42	0.43	0.53	0.55	0.45	0.58	0.50	0.58
	JJA	0.49	0.23	0.46	0.50	0.53	0.69	0.50	0.58
	SON	0.44	0.43	0.41	0.43	0.41	0.57	0.46	0.51
	DJF	0.30	0.19	0.39	0.41	0.28	0.51	0.36	0.45
l) NEACOF	MAM	0.29	0.11	0.36	0.28	0.22	0.43	0.30	0.40
	JJA	0.16	0.12	0.11	0.20	0.24	0.29	0.20	0.31
	SON	0.25	0.26	0.30	0.29	0.26	0.26	0.28	0.38
	DJF	0.09	0.06	0.17	0.30	0.15	0.26	0.19	0.29
m) ASEANCOF	MAM	0.49	0.45	0.54	0.57	0.46	0.61	0.53	0.62
	JJA	0.47	0.30	0.33	0.29	0.51	0.56	0.43	0.54
	SON	0.51	0.45	0.53	0.50	0.44	0.56	0.51	0.57
	DJF	0.41	0.24	0.46	0.50	0.35	0.61	0.45	0.56

Table 3. TCC of precipitation for MAM, JJA, SON and DJF over 13 RCOF regions for each single model and MME. Shading indicate 95% level of confidence, respectively.

		Model 1	Model 2	Model 3	Model 4	Model 5	Model 6	MEAN	MME
a) GHACOF	MAM	0.15	0.03	0.06	0.03	0.04	0.18	0.08	0.07
	JJA	0.03	-0.01	-0.05	-0.07	0.03	0.10	0.00	-0.03
	SON	0.21	0.04	0.03	0.05	0.15	0.20	0.11	0.09
	DJF	0.14	0.04	0.11	0.12	0.12	0.21	0.13	0.17
b) SARCOF	MAM	0.04	0.07	0.02	0.06	-0.01	0.15	0.06	0.09
	JJA	0.01	-0.01	-0.02	0.01	0.05	0.09	0.02	0.02
	SON	0.12	0.08	-0.02	0.00	0.01	0.14	0.05	0.06
	DJF	0.11	0.02	0.13	0.18	0.15	0.24	0.14	0.19
c) PRESAO	MAM	0.16	0.19	0.31	0.32	0.29	0.40	0.29	0.39
	JJA	0.15	0.15	0.10	0.11	0.27	0.32	0.20	0.31
	SON	0.14	0.11	0.29	0.27	0.25	0.34	0.25	0.34
	DJF	0.21	0.17	0.27	0.31	0.30	0.42	0.30	0.40
d) FOCRAII	MAM	0.17	0.12	0.23	0.24	0.22	0.31	0.23	0.32
	JJA	0.07	0.05	0.10	0.06	0.13	0.24	0.12	0.20
	SON	0.16	0.05	0.22	0.21	0.22	0.29	0.21	0.33
	DJF	0.16	0.11	0.20	0.24	0.19	0.33	0.22	0.31
e) WCSACOF	MAM	0.06	0.08	0.15	0.12	0.02	0.12	0.10	0.15
	JJA	0.09	0.09	0.08	0.04	0.11	0.22	0.12	0.19
	SON	0.13	0.02	0.15	0.17	0.10	0.20	0.14	0.19
	DJF	0.12	0.11	0.17	0.17	0.14	0.22	0.16	0.21
f) SSACOF	MAM	-0.03	0.14	0.18	0.18	0.10	0.18	0.14	0.23
	JJA	0.08	0.05	0.11	0.17	0.20	0.29	0.17	0.27
	SON	0.00	-0.03	0.16	0.20	0.18	0.23	0.14	0.22
	DJF	-0.08	0.04	0.15	0.11	0.13	0.17	0.10	0.17
g) PICOF	MAM	0.17	0.15	0.45	0.46	0.45	0.51	0.39	0.53
	JJA	0.23	0.21	0.21	0.21	0.43	0.44	0.32	0.48
	SON	0.46	0.21	0.56	0.48	0.61	0.54	0.50	0.64
	DJF	0.34	0.19	0.52	0.54	0.50	0.56	0.47	0.59
h) CACOF	MAM	0.09	0.11	0.13	0.15	0.08	0.15	0.13	0.19
	JJA	0.31	0.09	0.22	0.17	0.23	0.38	0.24	0.28
	SON	-0.05	0.23	0.23	0.09	0.09	0.41	0.18	0.23
	DJF	0.22	0.13	0.17	0.38	0.21	0.29	0.24	0.29
i) SEECOF	MAM	0.05	-0.04	-0.06	0.09	0.05	0.16	0.05	0.06
	JJA	0.06	0.01	0.02	0.08	0.20	0.17	0.10	0.16
	SON	-0.01	0.10	0.04	0.03	-0.09	0.14	0.04	0.06
	DJF	0.05	0.02	-0.05	0.15	0.12	0.19	0.09	0.16
j) SASCOF	MAM	0.14	0.12	0.24	0.29	0.24	0.31	0.24	0.32
	JJA	-0.01	0.04	0.12	0.13	0.09	0.17	0.10	0.18
	SON	0.08	0.03	0.18	0.20	0.11	0.18	0.15	0.24
	DJF	0.15	0.08	0.09	0.13	0.09	0.26	0.14	0.21
k) CARICOF	MAM	0.22	0.10	0.24	0.24	0.11	0.31	0.21	0.28
	JJA	0.26	0.19	0.14	0.12	0.25	0.40	0.24	0.34
	SON	0.14	0.14	0.21	0.27	0.14	0.32	0.21	0.27
	DJF	0.41	0.38	0.42	0.51	0.36	0.53	0.45	0.54
l) NEACOF	MAM	0.08	0.04	0.08	0.02	0.01	0.12	0.06	0.09
	JJA	-0.01	0.02	0.05	0.05	0.03	0.08	0.04	0.09
	SON	-0.03	0.06	-0.03	0.06	0.01	0.06	0.03	0.07
	DJF	0.00	0.05	0.00	0.06	0.07	0.10	0.06	0.11
m) ASEANCOF	MAM	0.21	0.19	0.26	0.32	0.33	0.39	0.30	0.42
	JJA	0.17	0.05	0.10	-0.03	0.22	0.32	0.15	0.24
	SON	0.31	0.08	0.39	0.34	0.36	0.44	0.35	0.50
	DJF	0.21	0.16	0.31	0.36	0.29	0.42	0.31	0.42

- (Table 2) As was already noted earlier (Wang *et al.*, 2009), the highest skill of 2m temperature seasonal prediction characterizes the areas affected by the El Nino Southern Oscillation (ENSO). Over these area (regions of PICOF and CACOF) and exceed the 95% confidence level both in the case of the MME and single model predictions. The MME predictions for other tropical regions (GHACOF and PRESAS) are also quite successful. The level of correlations for these RCOF regions is lower however. The lowest skill of the MME predictions characterizes the regions where the ENSO influence is low (SSACOF and NEACOF). Although MME provides an improvement of the forecast accuracy versus single models, predictions for these regions are characterized by a lower skill.
- (Table 3) Overall, these values are lower than those of the 2mtemperature. Nevertheless, the MME forecasts show higher skill for PICOF and ASEANCOF regions, as well as statistically significant MME values for all seasons over the PRESAO region.

Real-time forecast

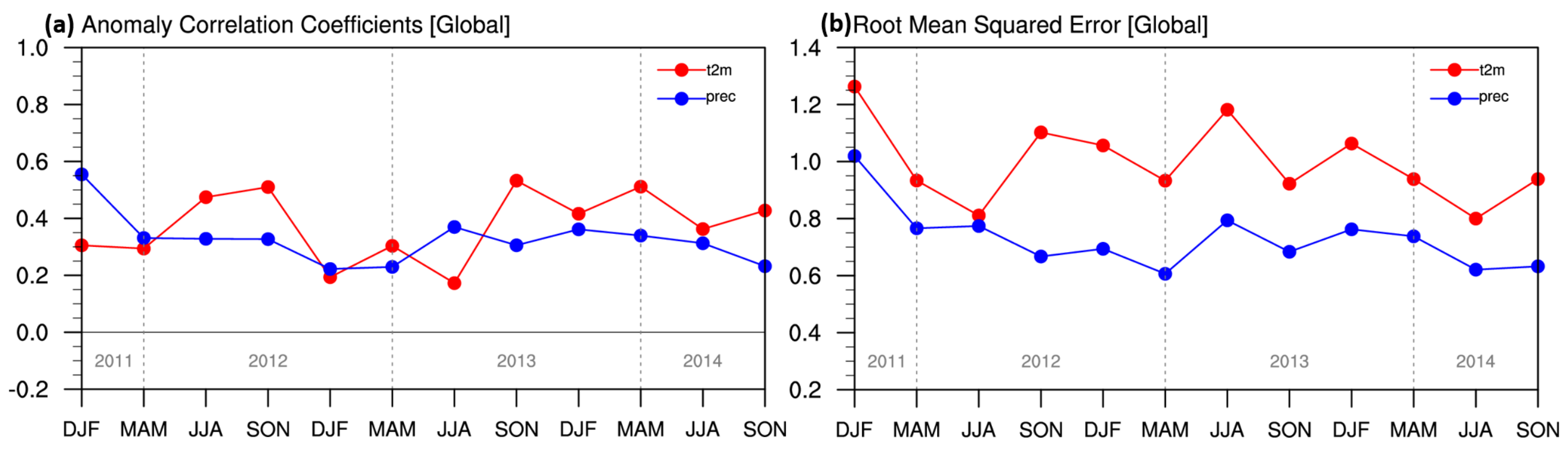

Fig. 4. Time series of (a) anomaly pattern correlation and (b) root mean squared error for seasonal mean temperature (red) and precipitation (blue) obtained from simple composite means for the period of DJF 2011/12-SON 2013 globally.

- The averaged ACCs for this period are 0.38 for 2m temperature and 0.33 for precipitation. For the RMSEs, the averaged skills are 0.73 for temperature and 1.00 for precipitation. That is, real-time operational MME forecasts of precipitation slightly outperform MME historical forecasts based on outputs from six models considered in this study. Note that the independent real-time forecasts (DJF 2011/12-SON 2014) are from operational predictions.

Summary and conclusion

- The GPC models represent higher seasonal prediction skill for temperature and precipitation in tropical regions, as well as better skills for temperature than for precipitation in the mid-latitudes.
- The prediction skills for an anonymous individual models and the MME over 13 RCOF regions for four seasons.
- The MME shows better seasonal prediction skill than the individual models, although the skills vary with season and region. The highest skill is demonstrated for the regions of the tropical RCOFs such as PICOF, ASEANCOF and CACOF, which were strongly affected by the ENSO. Additionally, the extratropical SSACOF and NEACOF regions show relatively low skills for all seasons compared to the other regions.
- The prediction skill of the MME is generally higher than that of the individual models. Thus, many operational centres [e.g. WMO LC-LRFMME, APCC, ECMWF, IRI, NCEP, MSC, and NMME] utilize the MME prediction system. However, it should be noted that the MME prediction skills are relatively limited. Specifically, the MME skills tend to originate from skillful models that successfully reproduce the dynamic processes, such as the tropical Pacific ENSO–rainfall relationship (Lee *et al.*, 2011, 2013a, 2013b).

References

- Hagedorn R, Doblas-Reyes F J and Palmer T N. 2005. The rationale behind the success of multi-model ensembles in seasonal forecasting - I. Basic concept. Tellus 57A: 219-233.
- Lee D-Y, Ashok K and Ahn J-B. 2011. Toward enhancement of prediction skills of multimodel ensemble seasonal prediction: A climate filter concept. J. Geophys. Res. 116: D06116. doi:10.1029/2010JD014610.
- Lee D-Y, Ahn J-B and Ashok K. 2013a. Improvement of Multimodel Ensemble Seasonal Prediction Skills over East Asian Summer Monsoon Region Using a Climate Filter Concept. J. Appl. Meteor. Climatol. 52: 1127-1138.
- Lee D-Y, Ahn J-B, Ashok K and Alessandri A. 2013b. Improvement of grand multi-model ensemble prediction skills for the coupled models of APCC/ENSEMBLES using a climate filter. Atmosph. Sci. Lett. 14: 139–145. doi: 10.1002/asl2.430
- Wang B, Lee J-Y, Shukla J, Kang I-S, Park C-K and coauthors. 2009. Advance and prospectus of seasonal prediction: Assessment of APCC/CliPAS 14-model ensemble retrospective seasonal prediction (1980-2004). Clim. Dyn. 33: 93-117.

Gayoung Kim (chorong@apcc21.org)

7th International Verification Methods Workshop

Berilin, Germany, May 3-11

Evaluation of Heat Wave forecasting using large-scale circulation pattern based on TIGGE data

Hyun-Ju Lee · Woo-Seop Lee · Jinho Yoo
APEC Climate Center(APCC), Busan, South Korea
asteria1104@apcc21.org

Introduction

As climate change, extreme weather events such as heat waves, droughts, heavy rain/snow, storms/floods have become more frequent and severe all around the world. In the future, high temperatures or heat waves are expected to occur more intensely and longer lasting due to global warming (Meehl and Tebaldi, 2004).

During the summer of 2003, a severe heat wave in Europe caused more 35,000 heat-related mortalities in many countries and had lost above 13 billion dollars. In 2010, western Russian experienced an intense heat wave that were 33 consecutive days above 30℃. Total economic losses are estimated 15 billion dollars due to wild fire and drought (Alexander, 2011).

A better understanding of the large scale connections is essential to improve the forecasts of heat wave. Lee and Lee(2016) found the inter-annual variability of summer heat wave and the large scale circulation patterns associated with the heat wave frequency in Korea during the past 40 years(1973~2012).

Matsueda(2011) showed that the ensemble forecast derived from multiple meteorological centres may actually perform better as compared to an ensemble derived from a single meteorological model in advance the potential occurrence of high-impact weather.

In this research, the goal is to analyze the atmospheric circulation features associated with heat wave of the year 2013. Also we investigated the occurrence probability of heat wave over Korea applying TIGGE(THORPEX Interactive Grand Global Ensemble) data for heat wave index associated with large scale circulation.

Analysis Method & Data

Definition of Heat Wave

The temperature exceeding the upper 95th percentile of the local climatological distribution and persisting for at least 2 days.

Heat Wave Index

We have used the Heat wave index proposed by Lee (APCC Tech. Report, 2013). The difference in 200hPa vorticity between the average over 25~30N, 110~130E and the average over 35~40N, 120~140E. When heat wave indices are greater than 0, it has probability to occur heat wave over Korea

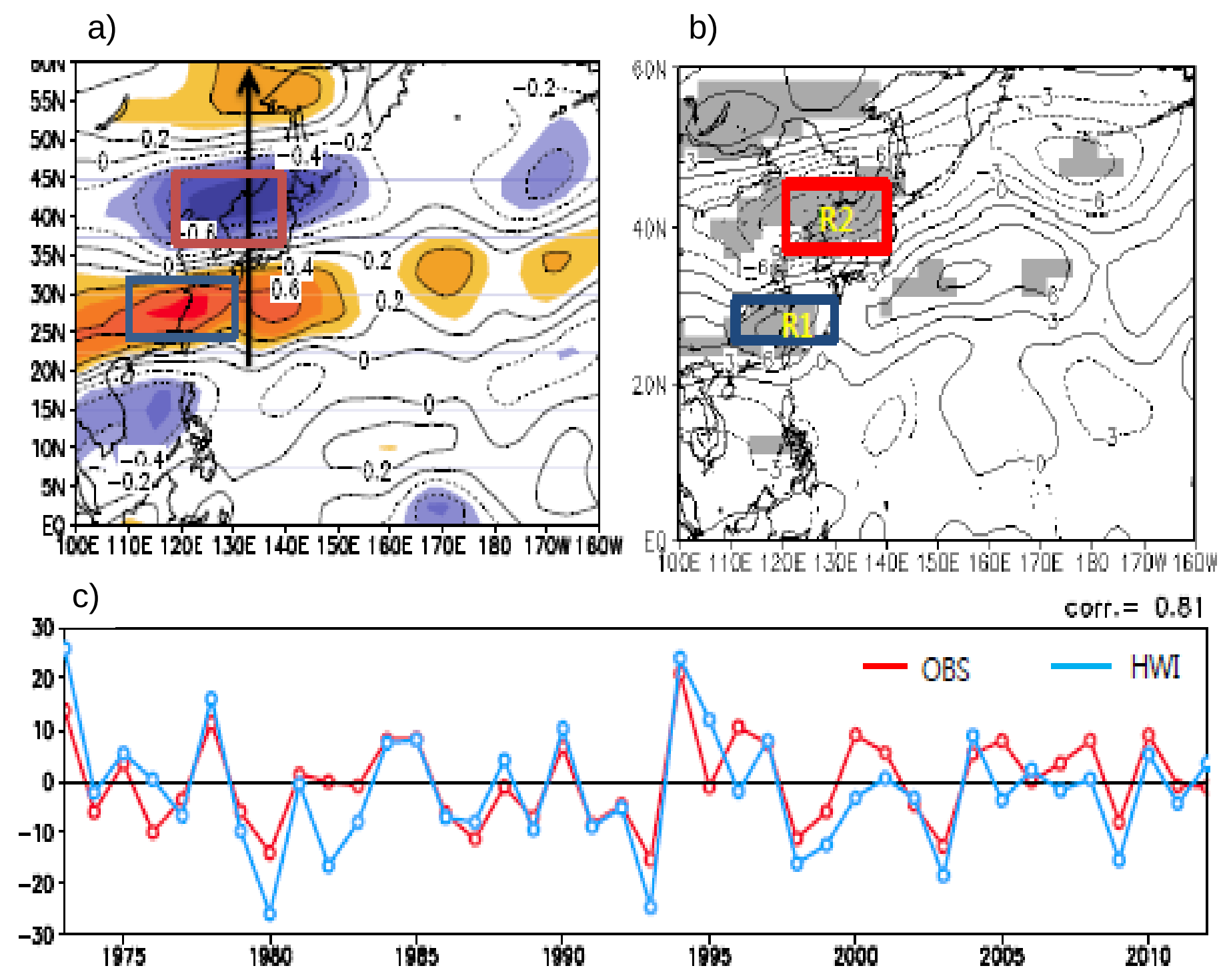

► Correlation patterns between PC1 of the Korean HWF and (a) 150hPa vorticity, (b) vorticity anomalies and (c) the time series of the PC1 (red) and HWI (blue) from 1973 to 2012 and heat wave index.

TIGGE(THORPEX Interactive Grand Global Ensemble) Data

	Country/Region	Center	Ensemble Members	Forecast length	Initial Perturbation	Model Resolution
(a)	USA	National Centres for Environmental Prediction (NCEP)	20	15day	Ensemble Transform with Rescaling	T126
(b)	Canada	Canadian Meteorological Centre (CMC)	20	15day	Ensemle Kalman Filter	TL213
(c)	Korea	Korea Meteorological Administration (KMA)	23	10day	Ensemble Transform Kalman Filter	N320
(d)	UK	Meteorological office (UKMO)	23	15day	Ensemble Transform Kalman Filter	N214
(e)	Europe	European Centre for Medium-Range Weather Forecasts (ECMWF)	50	10day	Singular Vectors	TL399

Reanalysis & Station Data

- NCEP II for u200, v200 and daily maximum temperatures (Kanamitsu et al. 2002)
- KMA ASOS for daily maximum temperatures

2013 Heat wave over Korea Korea

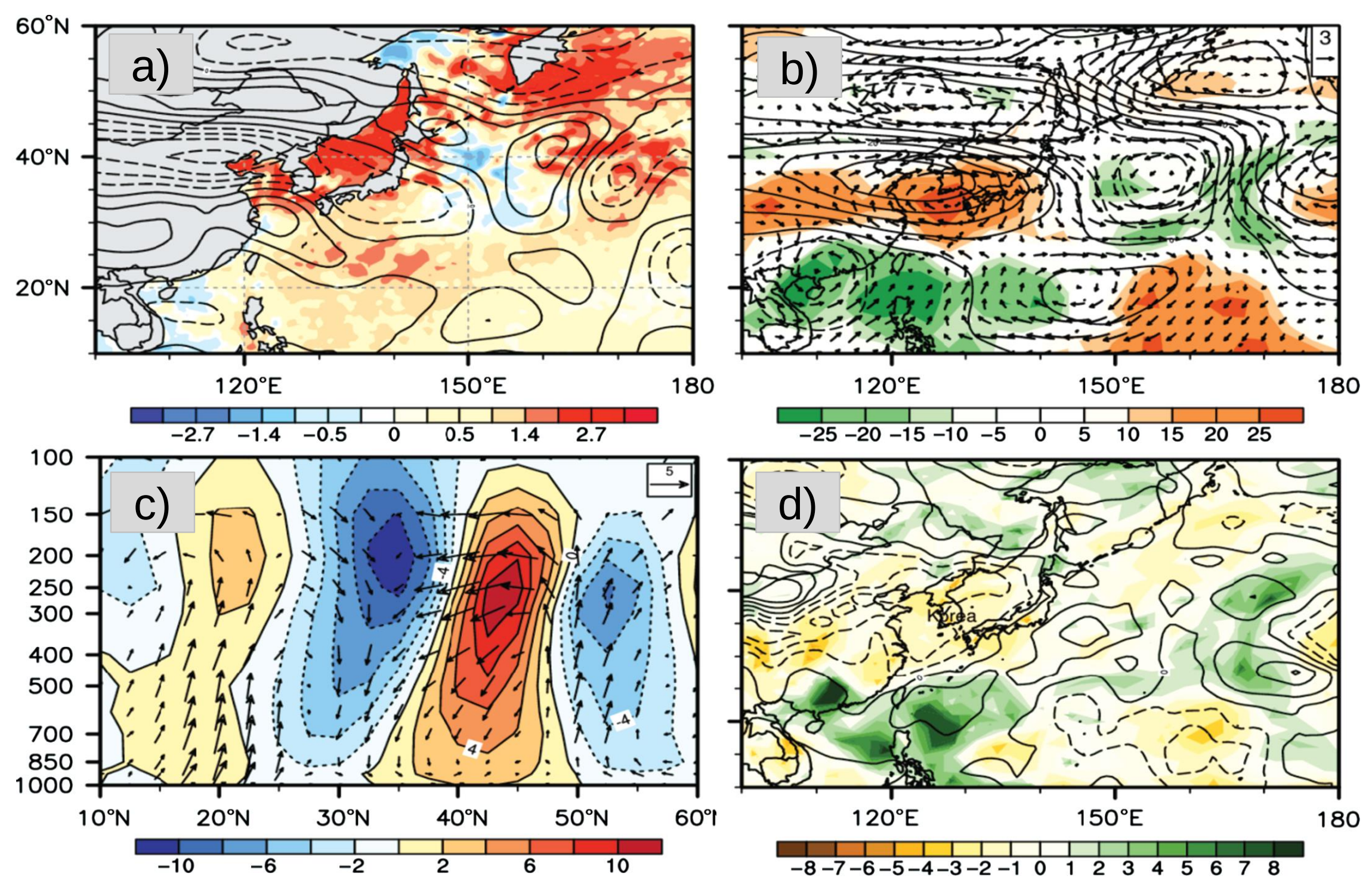

► (a) SST (shading, ∘C) and 200 hPa (contours, 10−6 s−1 interval) vorticity anomaly from 6 to 23 August 2013 for relative to 1981–2010. (b) Same as (a) but for outgoing longwave radiation (shading, Wm−2), 500 hPa geopotential height (contours, 10m interval) and 850 hPa wind (ms−1, arrows). (c) Meridional vertical circulation (vector) and zonal wind component (shading, ms−1) over 110∘ –130∘E. (d) Same as (a) but for precipitation (shading, mmday−1) and the rate of change of total cloud cover (contours, 10% interval) compared to 1981–2000.

- The North Pacific High expanded westward and the SSTs around Korea were significantly higher than normal. A noteworthy feature exhibited in the results is the north-south dipole mode that dominated the variability in the South China Sea, with opposite signs in the East Asia sectors. The positive anomaly of vorticity at 200 hPa over the South China Sea induced more convection and adiabatic heating, which in turn became a source of Rossby wave-train along southerly wind patterns that generated positive geopotential height anomalies around Korea.

Heat Wave Forecast

❖ Forecast for Heat Wave

1) **TMAX** (Maximum Temperature) : forecast of heat waves when the daily maximum temperature exceeds the upper 95th percentile value of the observed climatological PDF
2) **BCT** (Bias Corrected Temperature) : forecast of heat waves when the daily maximum temperature exceeds the value of the upper 95th percentile of each model's climatological PDF
3) **HWI** (Heat Wave Index) : forecast of heat waves when the HWI, which is based on large-scale circulation, is positive.

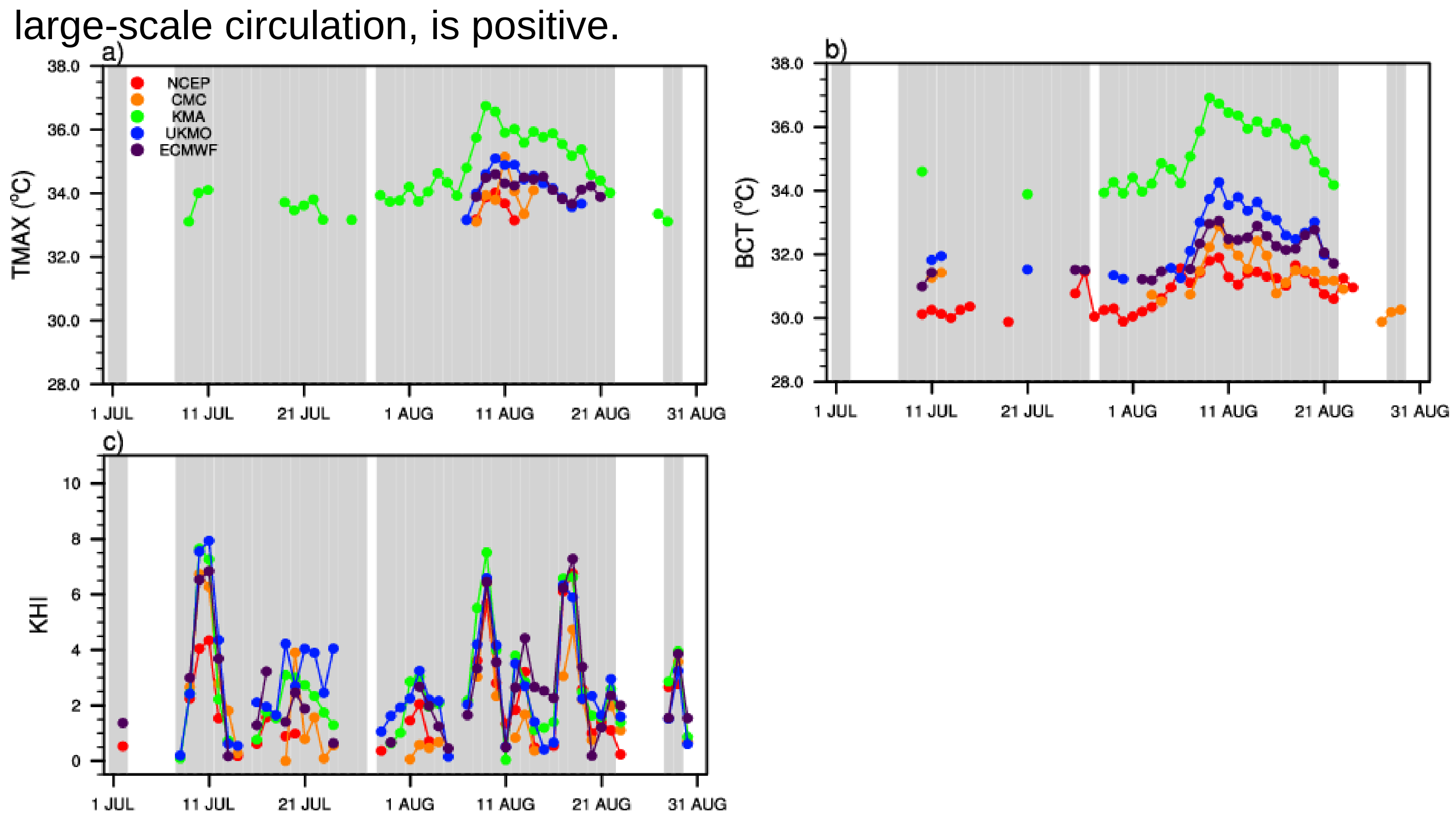

- When using TMAX, all models failed to forecast heatwave events(The shading indicates the occurrence of an observed heat wave), particularly in early summer.
- However, when the bias correction is applied, all the models show very similar results, but they do fail to predict the occurrence of heat waves in early summer.
- Compared to the other two methods determined by temperature, forecasting with HWI is able to forecast early summer heat waves well.

❖ Verification

		Event observed		
		Yes	No	
Event forecast	Yes	**Hit (H)**	**False (F)**	Yes fcsts (H+F)
	No	**Miss (M)**	**Correct Negative (N)**	No fcsts (M+N)
		Yes obs (H+M)	No obs (F+N)	Total (H+F+M+N)

- $PC = \frac{H+N}{H+F+M+N}$

0~1 (1: Perfect skill)

- $CSI(TS) = \frac{H}{H+F+M}$

0~1 (1: Perfect skill)

- $ETS = \frac{H}{H+F+M} - H_{ref} = \frac{H-H_{ref}}{H+F+M-H_{ref}}$

–1/3~ 1 (0: No skill, 1: Perfect skill)

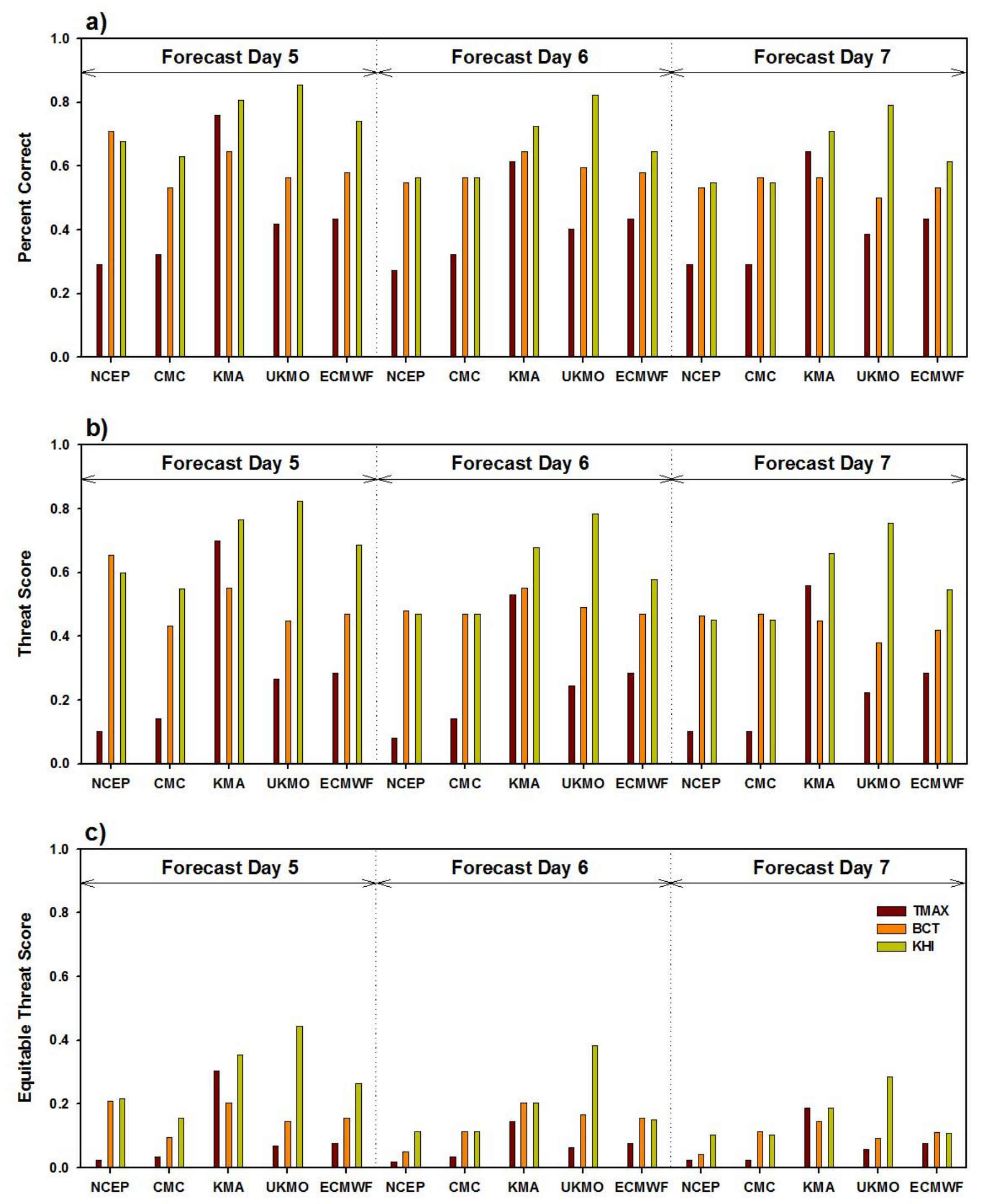

- The KMA has a greater than 0.7 in PC value, whereas NCEP, CMC, UKMO and ECMWF indicate less than 0.4 in PC. This shows that forecasting heat waves in July is difficult using daily maximum temperature.
- The forecast of heat waves using BCT is more realistic than that using TMAX.
- The verification of the PC and the TS showed that the heat-wave forecast using HWI compared to others regardless of forecast time was successfully carried out. HWI is able to provide an early warning forecast for heat waves with 5 days up to 9 days forecast.

Conclusion

In this study,

- we analyzed the atmospheric circulation features associated with heat wave of 2013 summer.
- We found that the strengthening of the Northwestern Pacific High resulting from the anomalous convergence over South China contributes to the intensification of the heat wave during heat wave in 2013.
- Based on the TIGGE datasets, The highest skill in forecasting the heat waves was given by HWI even during the period from 8 to 27 July, when it had a lower probability, compared to the others two methodologies (BCT, TMAX). For all lead times, all of the PC, TS and ETS of HWI were higher than those of BCT and TMAX. Results in predicting a heat-wave occurrence by HWI indicates significant skill in both short and medium-range.
- These results might help us to get reliable information about heat waves in advance and this can provide more prevention time for the public in Korea.
- advanced planning and preparedness are essential and can reduce the health impacts of exposure to extreme climate events like heat wave.

Reference

- Alexander L., 2011: Extreme heat rooted in dry soils, Nat. Geosci. 4, 12-13.
- Lee W-S and M.I Lee. 2016 : Interannual variability of heat waves in South Korea and their connection with large-scale atmospheric circulation patterns. *Int. J. Climatol.*, **36**, 4815–4830, doi:10.1002/joc.4671.
- Matsueda M. 2011. Predictability of Euro-Russian blocking in summer of 2010. Geophysical Research Letters 38: L06801, doi: 10.1029/2011GL046557.
- Meehl G.A., Tebaldi C., 2004: More intense, more frequent, and longer lasting heat waves in the 21st century. Science 303, 1499-1503.

7th International Verification Methods Workshop, in Berlin, Germany, 3-11 May, 2017

Verification for long-lead station-scale prediction of hydrological droughts in South Korea based on bivariate pattern-based downscaling

Soo-Jin Sohn[1], and Chi-Yung Tam[2]

[1]APEC Climate Center, Busan, Republic of Korea

[2]Earth System Science Programme, The Chinese University of Hong Kong, Hong Kong, China

Background

- **Capturing climate variations in boreal winter to spring (December-May) is essential for properly predicting droughts in South Korea.**

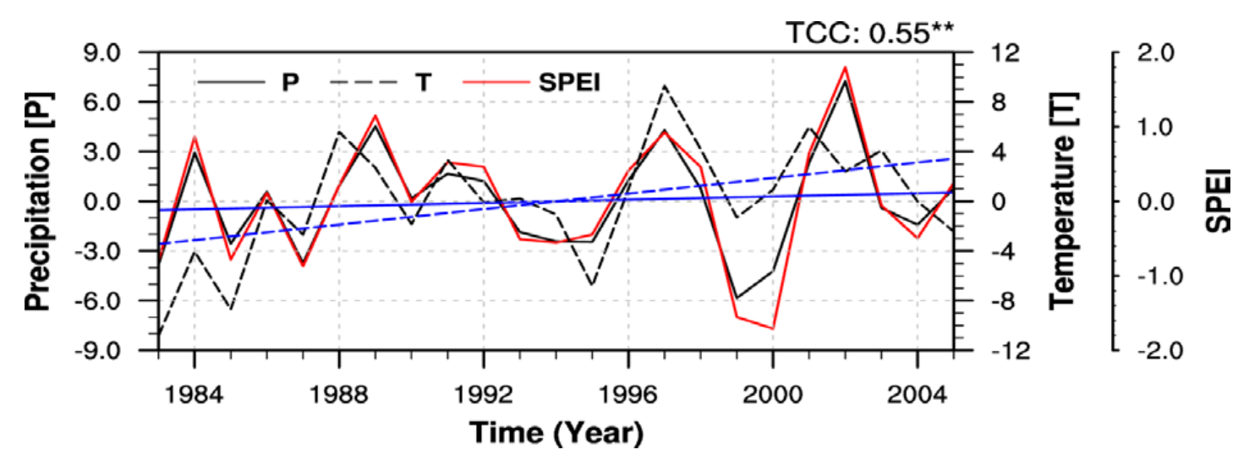

Fig. 1 Time series of the observed December to May anomalous precipitation (black solid line), surface air temperature (black dashed line), and the standardized precipitation evapotranspiration index (SPEI) (red solid line) during the 1983/1984 to 2005/2006 period, averaged over 60 station locations in South Korea. The correlation between the former two time series exceeds the 99% significance level, and its value is given in the upper right. Solid and dashed straight lines (in blue) show the linear trend of the precipitation and temperature measurement, respectively.

- **Winter-to-spring seasonal mean surface temperature and precipitation in South Korea are positively correlated with each other**
- **A robust warming trend is present in the recent climate records over this region**

→ It thus seems imperative to incorporate both temperature and precipitation effects on drought occurrences over South Korea

Data and Methodology

1. Data

Table Description of the nine climate models used in this study.

Country	Institute	Model	AGCM/resolution	OGCM/resolution	Ensemble Member	Reference
Australia	BOM	POAMA2.4	BAMv3.0d/T47L17	ACOM2/0.5-1.5°lat x 2°lon L25	10	Cottrill et al. (2013)
Canada	MSC	CCCma CGCM3	AGCM3/T63L31	OGCM4 (1.41°lon x 0.94°lat L40)	10	
	MSC	CCCma CGCM4	AGCM4/T63L31		10	
Korea	APCC	CCSM3	CAM3/T85L26	POP1.3/Gxlv3_L40	5	Jeong et al. (2008)
	PNU	PNU	CCM3/T42L18	MOM3/0.7~2.8 lat L29	10	Sun and Ahn (2011)
	SNU	SNU	SNU/T42L21	MOM2.2/⅓°lat x 1°lon L32	6	Ham and Kang (2010)
USA	NASA	GMAO	GEOS-5/288x181L72	MOM4/720 x 410 L40	9	
	NCEP	CFS	GFS/T62L64	MOM3/⅓°lat x 1°lon L40	15	Saha et al. (2006)
	UH	UH	ECHAM4/T31L19	UH Ocean/1°lat x 2°lon L2	10	Fu and Wang (20004)

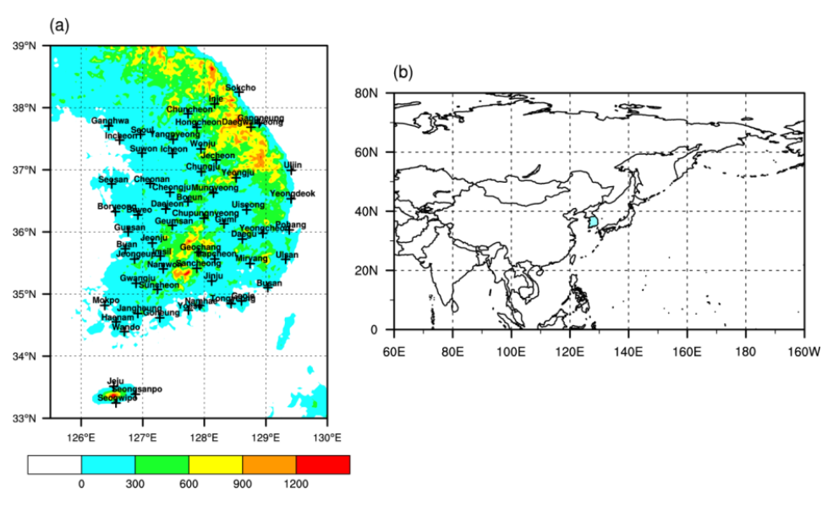

Fig. 2 (a) Topographic map (shaded; units: m) with the locations of 60 stations (marked with crosses) and (b) predictor domain with South Korea indicated by shading considered in this study.

2. Methodology

1. Data Compression

: A key feature of this analysis involves **concatenating spatial fields of predictand data from two different variables**

→ Define both the **space and time evolution** of the climate system

→ Consider **inter-variable coherence**

- The composite predictand set (T') would be defined by

$$T'(x',\mathrm{t}) = \begin{cases} P(t,\eta) & x' = 1,2,\cdots,m; \quad \eta = 1,2,\cdots,m \\ T(t,\eta) & x' = m+1,2,\cdots,2m; \quad \eta = 1,2,\cdots,m \end{cases}$$

where $\mathrm{t} = 1,2,\cdots,\mathrm{n}$ and $x' = 1,2,\cdots,2m = q$

2. Prediction Equations

Predictor $Y(x,t) = \sum_{j=1}^{p} \kappa_j^{1/2}\, \alpha_j(t) e_j(x) \quad x = 1,2,\cdots,\mathrm{p}$

Predictand $\mathrm{T}(x',\mathrm{t}) = \sum_{j=1}^{q} \lambda_j^{1/2}\, \beta_j(t) f_j(x') \quad x' = 1,2,\cdots,\mathrm{q}$

3. Further can be found in **Barnett and Preisendorfer (1987)**

Dominant modes of winter-to-spring climate variability in South Korea

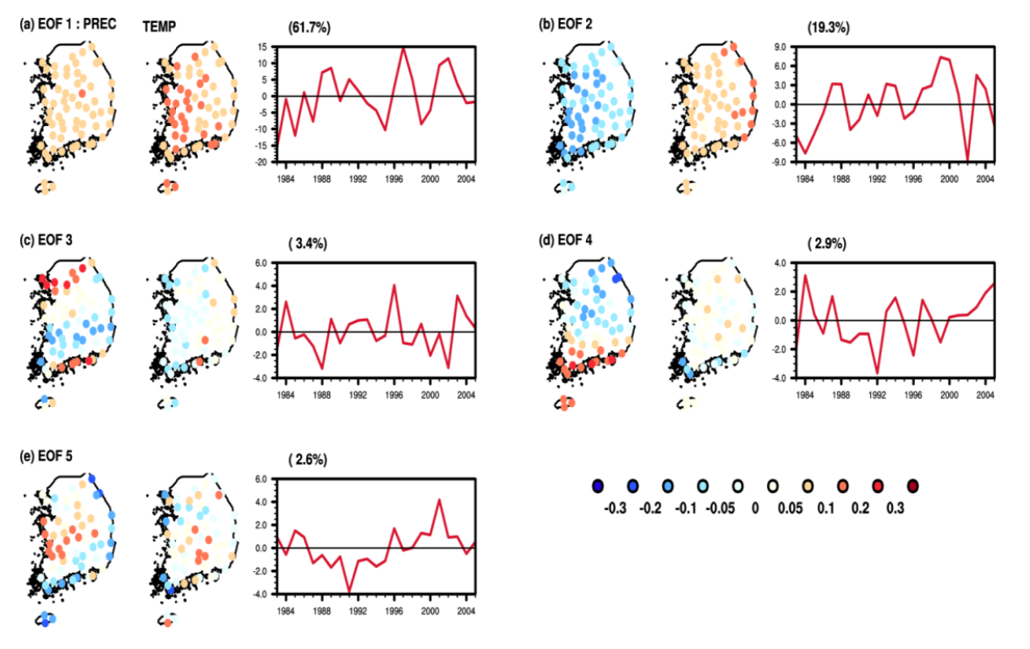

Fig. 3 The multivariate EOF patterns and time coefficients of the observed December to May anomalous precipitation and surface air temperature in South Korea during the 23 years from 1983/1984 to 2005/2006 for the (a) first, (b) second, (c) third, (d) fourth, and (e) fifth modes. The respective panels consist of spatial patterns of precipitation (left column) and surface air temperature (middle column) as well as PC time series (right column).

- **Multivariate empirical orthogonal function (EOF) analysis results based on observations show that the first two leading modes of winter-to-spring precipitation and temperature variability, which together account for ~80 % of the total variance, characterized by regional-scale anomalies covering the whole South Korean territory.**

Table Correlation coefficients between the first and second PC time series and various climate indices computed using accumulated values within the whole December to May period, from 1983/84 to 2005/2006 based on observations. Values exceeding the 99% significance level are marked by double asterisks and those exceeding the 95% significant level are marked by single asterisks.

Indices	PC 1	PC 2
NAO	0.07	0.33
EA	0.43*	0.20
WP	0.62**	0.16
EP/NP	0.32	0.07
PNA	-0.38	0.09
EA/WR	0.71**	-0.03
SCA	-0.36	-0.44*
POL	0.21	-0.43*
AO	0.44*	0.16
SH	-0.59**	-0.43*
Nino3	0.44*	0.13

- **These modes were closely related to some of the recurrent large-scale circulation changes in the northern hemisphere during the same season.**

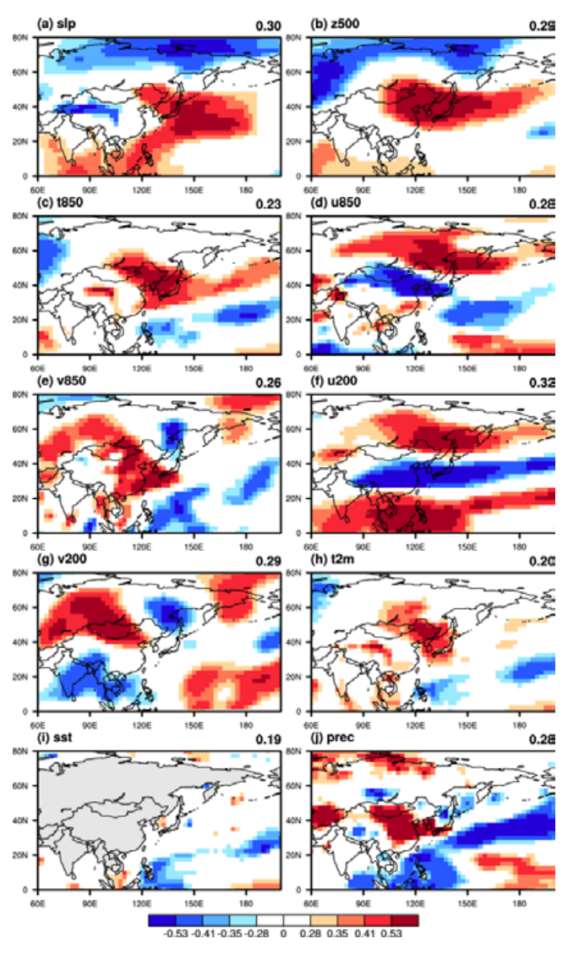

Fig. 4 Temporal correlation coefficients (TCCs) of the observed December to May anomalous potential predictors from (a) mean sea-level pressure (SLP; units: hPa), (b) 500hPa geopotential height (Z500; m) , (c) 850hPa temperature (T850; °C), (d) 850hPa meridional wind component (U850; m/s), (e) zonal wind component (V850; m/s), (f) 200hPa meridional wind component (U200; m/s), (g) 200hPa zonal wind component (V200; m/s), (h) 2m temperature (T2M; °C), (i) sea surface temperature(SST; °C), (j) precipitation (PREC; mm/day) with SPEI during the 1983/1984 to 2005/2006 period, over predictor domain. Shading denotes values exceeding the 80% significance. The area-average of absolute values over the domain are provided in upper right of each panel.

- **Examination of the standardized precipitation evapotranspiration index (SPEI) indicates that drought conditions in South Korea tend to be accompanied by regional-to-continental -scale circulation anomalies over East Asia to the western north Pacific.**

Objective and Strategy

- **Motivated by the aforementioned findings on**

the spatial-temporal coherence among stations-scale precipitation and temperature anomalies,

→ a new bivariate and pattern-based downscaling method was developed.

>> This study investigates the variability and predictability of the South Korean climate during this extended season, based on observations from 60 station locations and multi-model ensemble (MME) hindcast experiments (1983/1984-2005/2006) archived at the APEC Climate Center (APCC).

>> The novelty of this method is that precipitation and temperature data were first filter using multivariate EOFs to enhance their spatial-temporal coherence, before being linked to large-scale circulation variables using canonical correlation analysis (CCA).

Development of statistical prediction model for winter-to-spring climate and Verification for drought prediction

I. Perfect model based on observed linkage

- **To test its applicability and to investigate its related potential predictability, a perfect empirical model was constructed with observed datasets as predictors.**

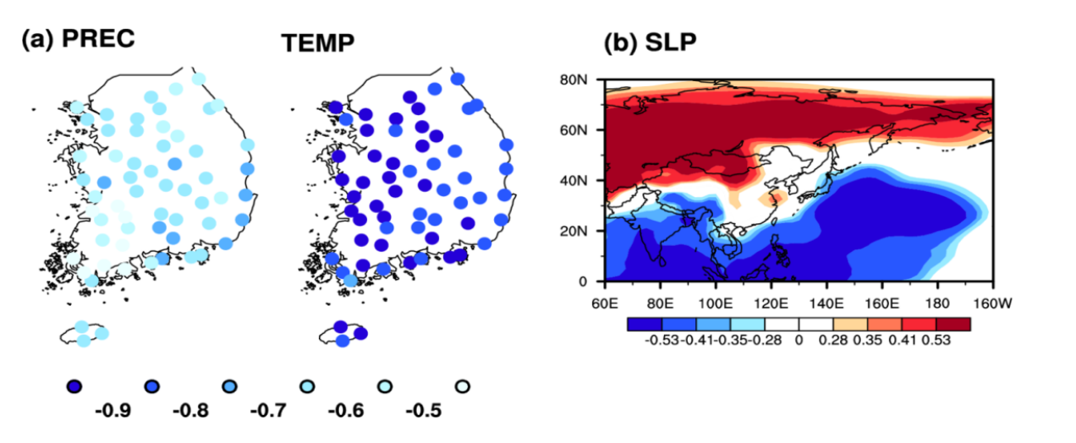

Fig. 5 Canonical maps of the observed December to May anomalous precipitation (left panel), surface air temperature (middle panel) over 60 station locations in South Korea, and simultaneous SLP in the predictor window. The canonical maps are vectors at specific location between predictand or predictor and their respective canonical component time series. These patterns explain 57% and 18% of the total variances for predictand and predictor, respectively. The correlation between the respective amplitude time series of these patterns is 0.86.

- **The dominant spatial pattern of interannual variability of the winter-to-spring precipitation and temperature is associated with a seesaw SLP structure between the southern and northern parts of East Asia.**

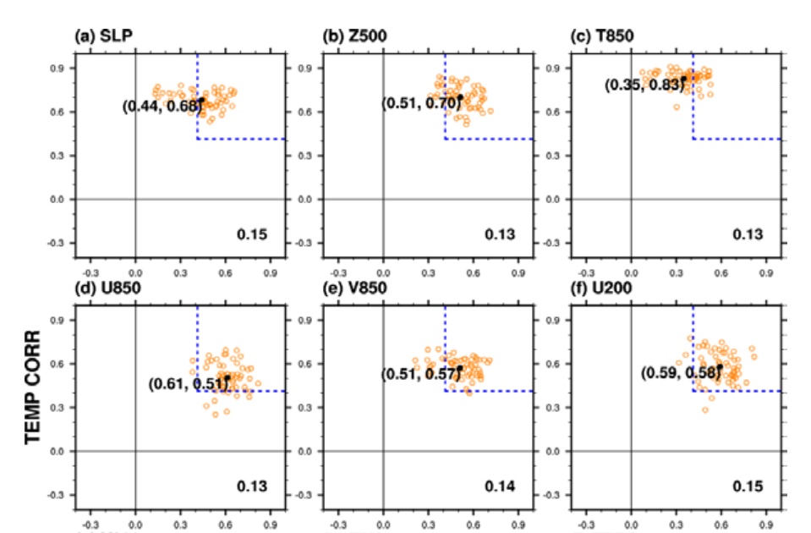

Fig. 6 Scatter plots of TCCs between the observed and predicted precipitation (x axis) and temperature (y axis), for the potential predictor of (a) SLP, (b) Z500, (c) T850, (d) U850, (e) V850, (f) U200, (g) V200, (h) T2M, and (i) PREC. Each orange point represents the results based on perfect model predictions for one station location. The black dots denote the TCC values averaged over 60 stations in South Korea. The rectangle in top right corner of each panel (partly surrounded by blue dot lines) denotes the zone exceeding the 95% significance for both of precipitation and temperature. The "standard distance deviation" of both of precipitation and temperature is given at the bottom right of each panel.

- **Forecast skills can vary greatly from one predictor to another.**

II. Dynamical vs. hybrid model

- **A model output statistics (MOS)-type hybrid dynamical-statistical model was developed, using products from nine one-tier climate models as inputs.**

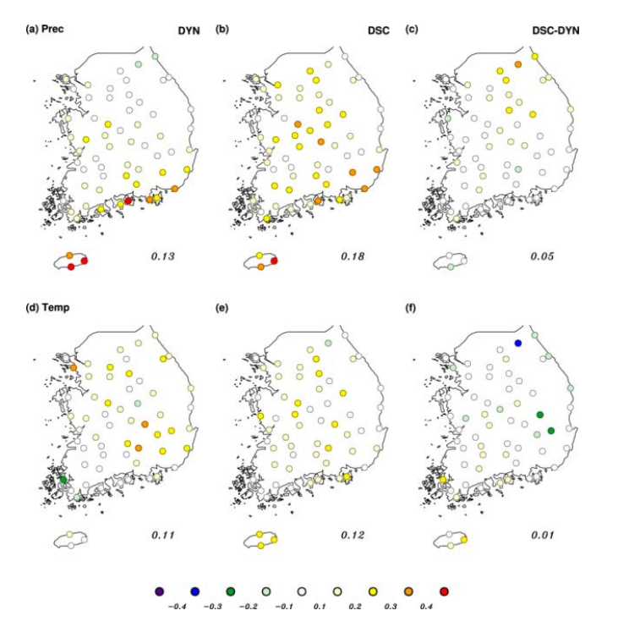

Fig. 7 TCCs between the observed and predicted (a, b, c) precipitation, and (d, e, f) temperature from December to May, from (a, d) raw mutlimodel ensemble (MME), (b, e) downscaled MME (DMME), and (c, f) and their difference for each station. The temporal correlation averaged over the 60 stations is given at the bottom right of each panel.

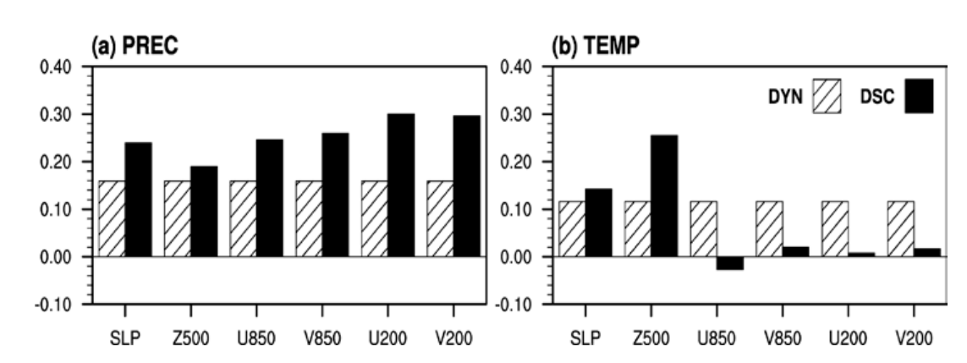

Fig. 8 TCCs between the observed and predicted (a) precipitation, and (b) temperature from December to May during the 1983/84 to 2003/2004 period, averaged over 60 stations locations in South Korea. Hatched bars denote raw MME and solid bars denote DMME.

- **With model sea-level pressure (SLP) and 500 hPa geopotential height (Z500) as predictors, statistically downscaled MME (DMME) precipitation and temperature prediction were substantially improved compared to those based on raw MME outputs.**

III. Limitation of hybrid model and its cause

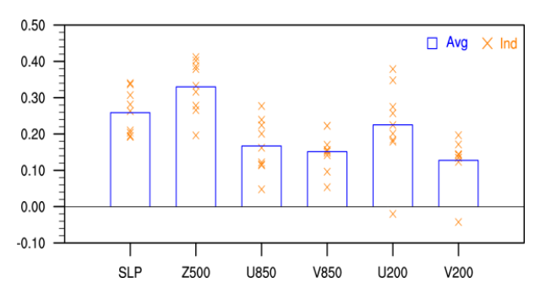

Fig. 9 TCCs between the observed and predicted December to May anomalous potential predictors, averaged over the predictor domain, during the 1983/84 to 2005/2006 period. Bars denote the average of individual models' skills and crosses denote single-model results.

- **The actual predictability did not quite reach the potential predictability as estimated from a perfect model**
- **Dynamical modes still have difficulties in capturing some detailed circulation features.**

IV. Prediction of winter-to-spring drought and its verification

- **The dynamical-statistical model was used to construct 6 month-lead drought predictions for 60 stations in South Korea.**

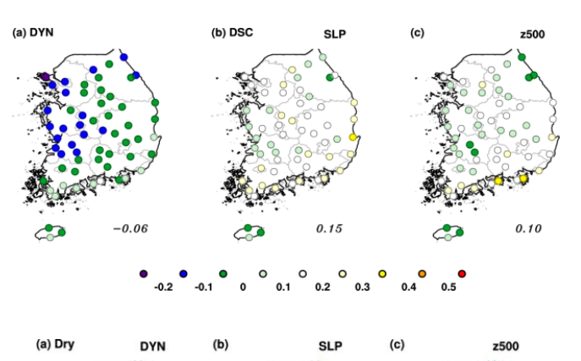

Fig. 10 The linear error in probability scores (LEPSs) between observations and predictions on (a) raw MME, and (b, c) inflated DMME predictions with (b) SLP and (c) Z500 as predictor, for SPEI6 during 1983/84 to 2005/06. The skill score averaged over 60 station locations is given at the bottom right of each panel. Grey lines indicate the boundaries of administrative areas for South Korea.

- **DMME was found to give reasonably skillful long-lead forecasts of SPEI for winter to spring.**
- **DMME-based products clearly outperform the raw MME predictions, especially during extreme wet years.**

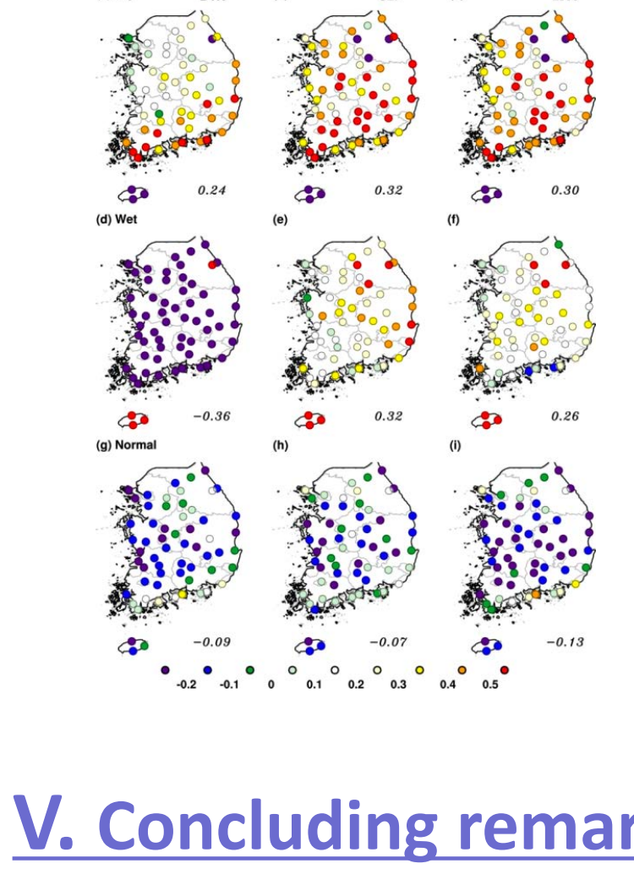

Fig. 11 The linear error in probability scores (LEPSs) between observations and predictions on (a, d, g) raw MME, and (b, c, e, f, i) inflated DMME predictions with (b, e, h) SLP and (c, f, i) Z500 as predictor, for SPEI6 during (a, b, c) dry, (d, e, f) wet, and (g, h, i) normal years.

V. Concluding remarks

- **Our results could lead to more reliable climatic extreme predictions for policymakers and stakeholders in the water management sector, and for better mitigation and climatic adaptations.**

VI. Reference

- **Sohn, S. & Tam, C. Clim Dyn (2016) 46: 3305. doi:10.1007/s00382-015-2770-3**

7th International Verification Methods Workshop
3-11 May 2017, Berlin, Germany

Asia-Pacific Economic Cooperation
Climate Center

Project #8:
Verification of deterministic precipitation forecasts

Eun-Hee Lee, Ki-Byung Kim
Korea Institute of Atmospheric Prediction Systems, Seoul

Soo-Jin Sohn, Hyun-Ju Lee, Gayoung Kim
APEC Climate Center, Pusan

Project #8
Verification of deterministic precipitation forecasts

Daily precipitation 3 day prediction data

- By the KIAPS Integrated Model (KIM)
  : non-hydrostatic global NWP model on the cubed sphere
  : Resolution ~25km
- JJA 2016, DJF 15/16

[Location of observation stations]

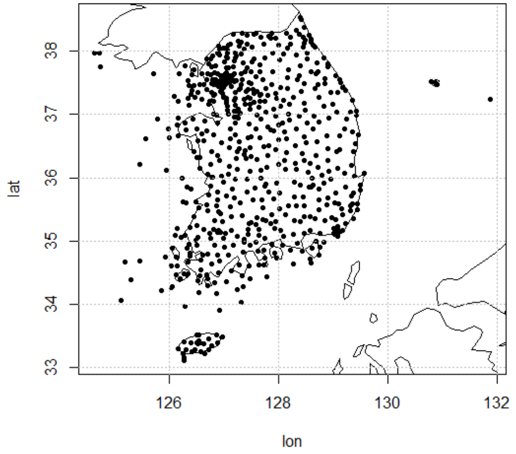

Observation

- Rain gauge data from 617 stations over Korean peninsula
- Daily accumulated from hourly prcp.

Verification

- Bilinear interpolation from model grid to obs. point
- Verified using contingency tables

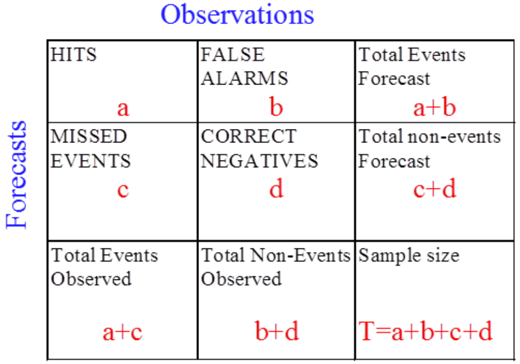

Observations

Forecasts

HITS a	FALSE ALARMS b	Total Events Forecast a+b
MISSED EVENTS c	CORRECT NEGATIVES d	Total non-events Forecast c+d
Total Events Observed a+c	Total Non-Events Observed b+d	Sample size T=a+b+c+d

JJA vs. DJF precipitation

Daily precipitation (all station averages)

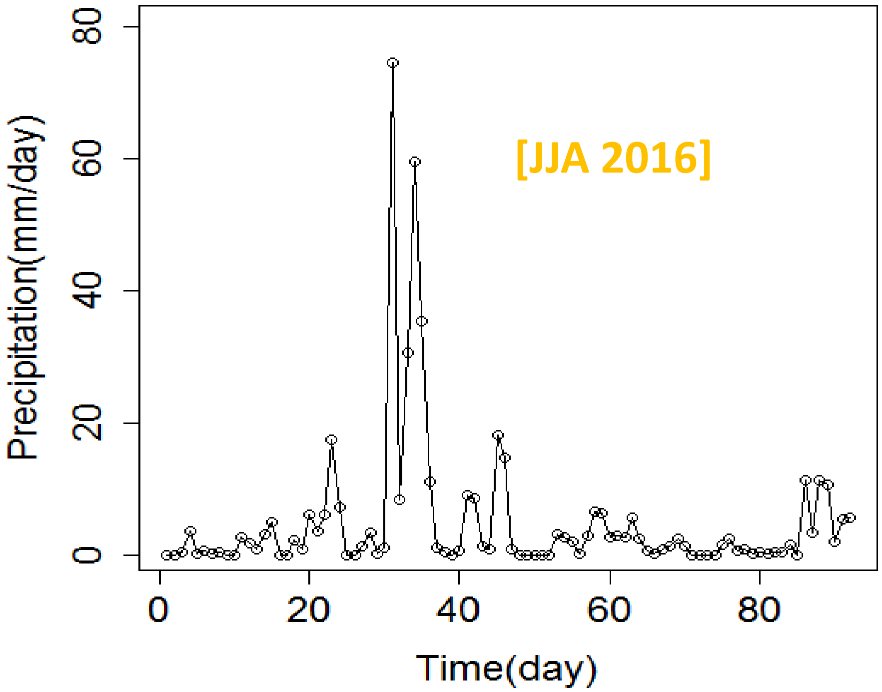

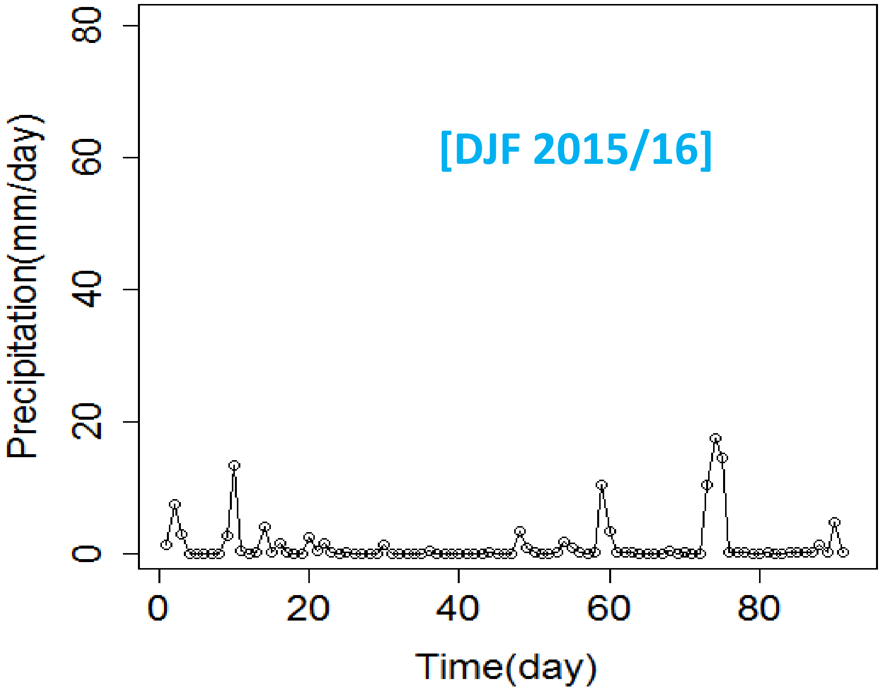

JJA ~ rainy, prevailing persistent monsoonal rain period
, followed by rainy days due to synoptic front, convective systems
DJF ~ relatively dry season, local rainy events..

Data

JJA16

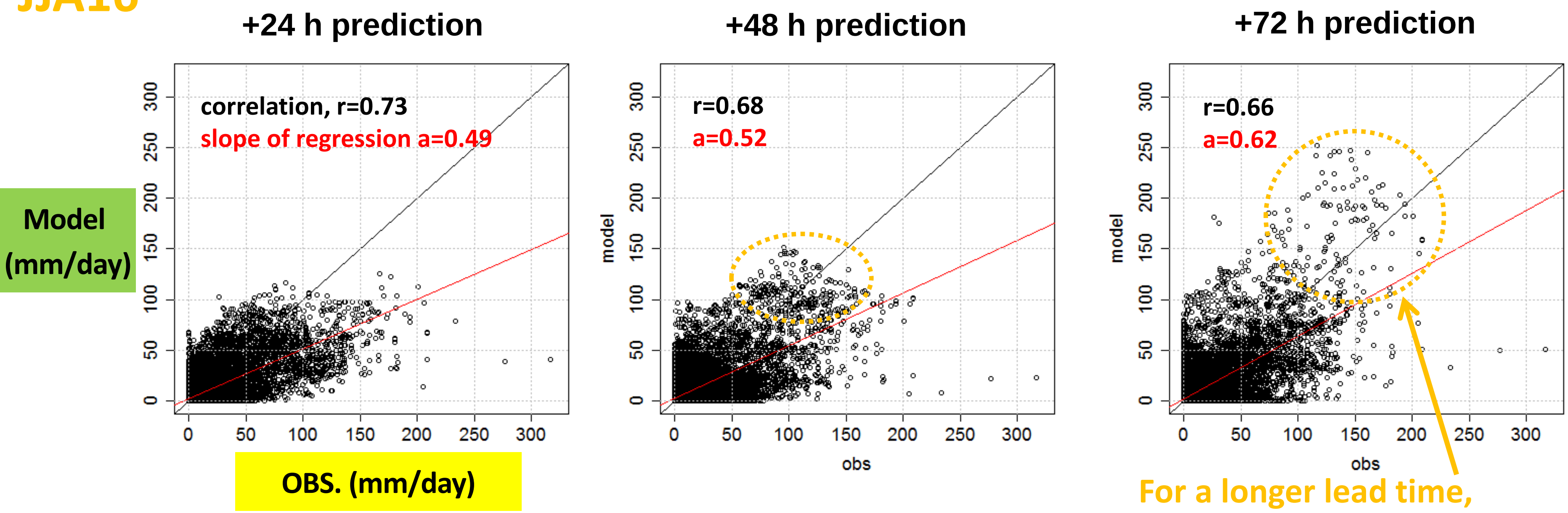

For a longer lead time, Model tends to intensify rain system for some events

DJF15/16

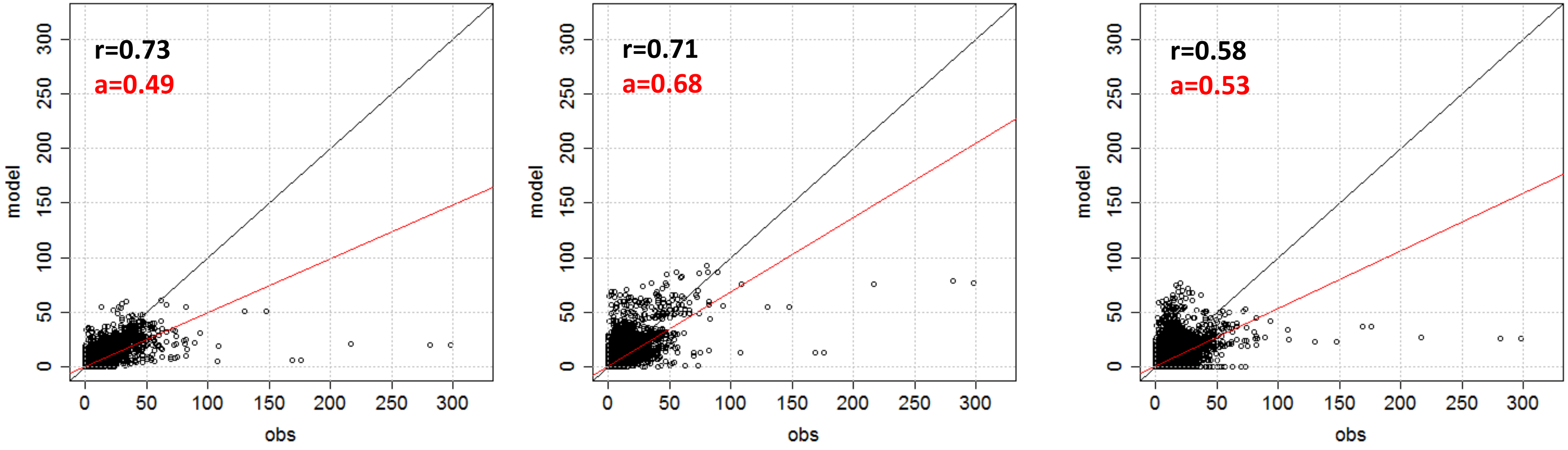

Data distribution & selected thresholds

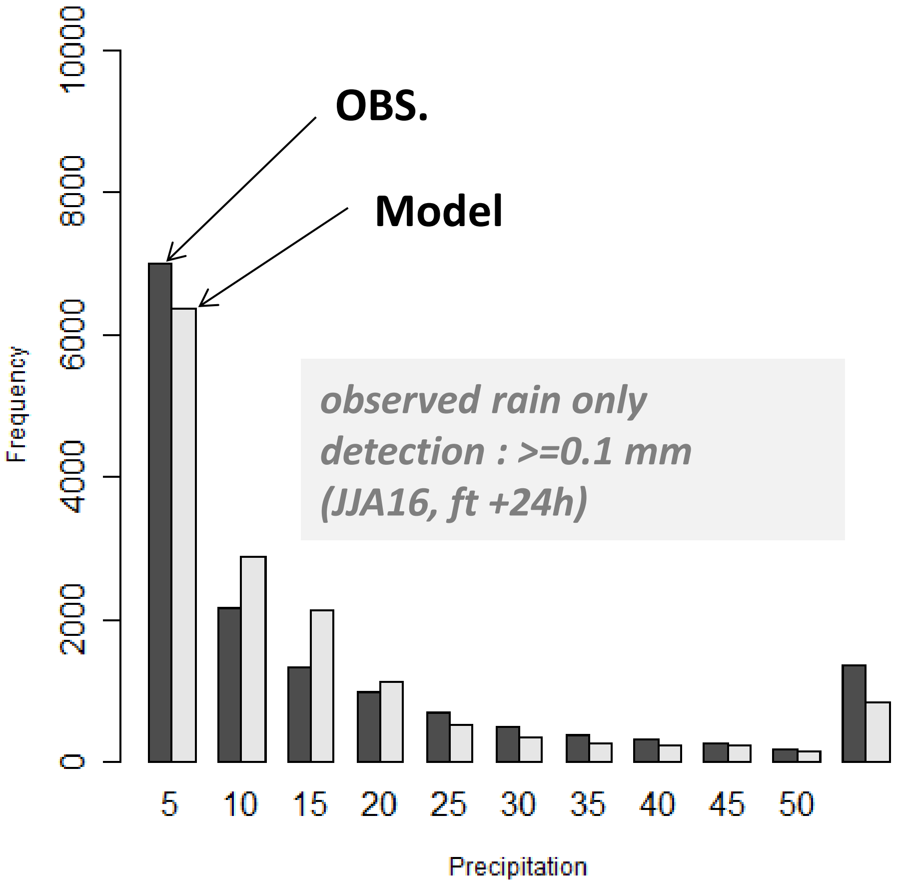

observed rain only detection : >=0.1 mm (JJA16, ft +24h)

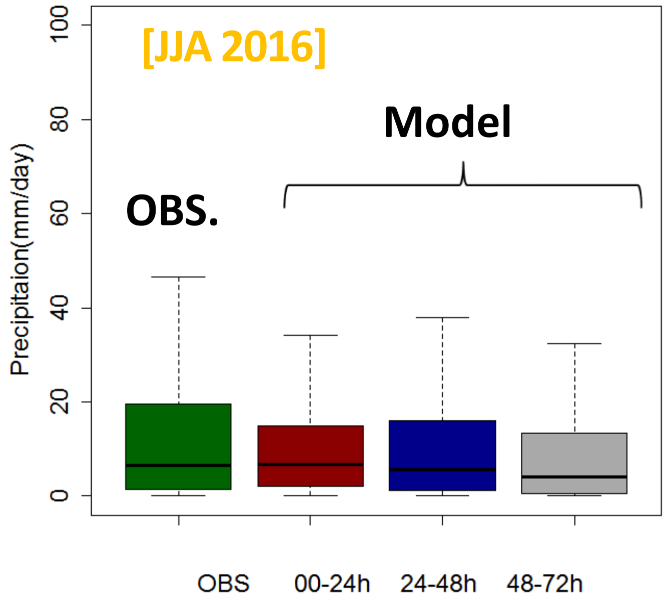

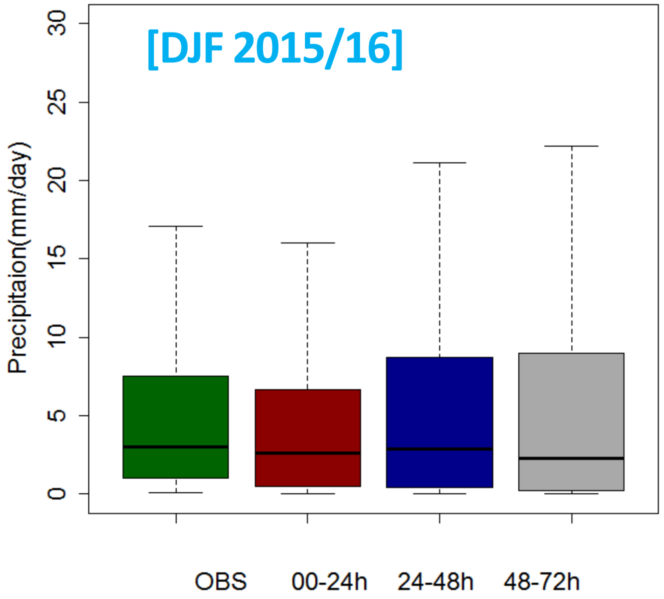

Thresholds for contingency table verification

Heavy rainfall warning by KMA: 110 mm/12hr

Lowest 0.5 mm, highest 100 mm/day

➔ 0.5, 2, 5, 10, 20, 30, 50, 100 mm/day

Verification results (+48 h prediction)

JJA

$$POD = \frac{hit}{obs.\text{"Yes"}}$$

$$FAR = \frac{false\ alarm}{Predicted\ \text{"Yes"}}$$

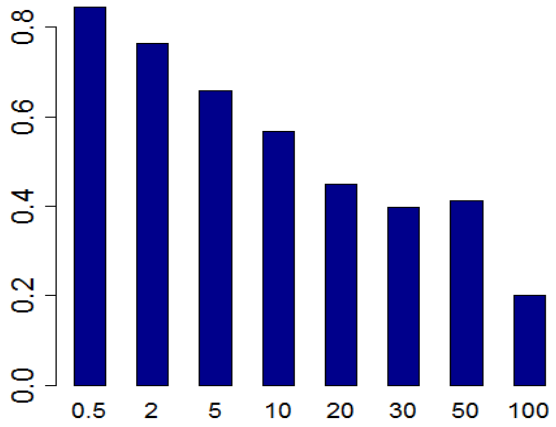
POD

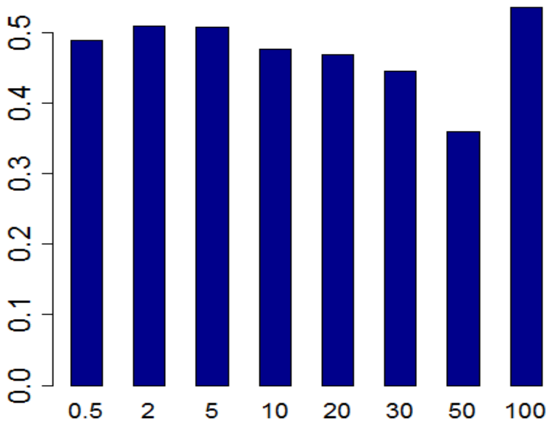
FAR

Higher false alarm ratio for smaller thresholds in JJA

Higher hit rate for light rain for both JJA and DJF

DJF

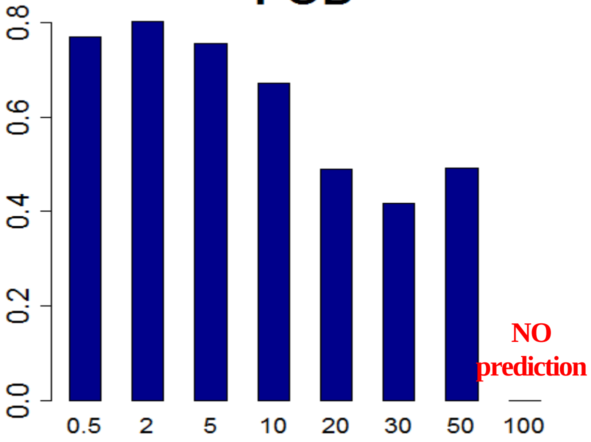
POD

NO prediction

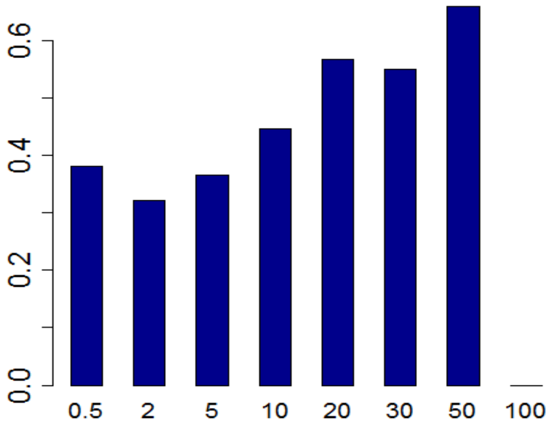
FAR

Higher false alarm ratio for heavier rain thresholds in DJF

Verification results (+48 h prediction)

$$BIAS = \frac{pred."Yes"}{obs."Yes"}$$

JJA

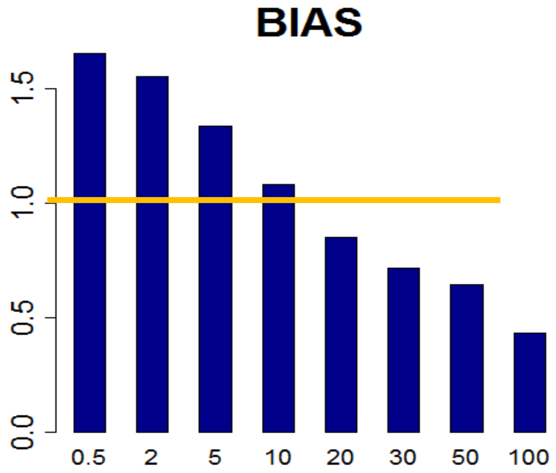

Over-predicted light rain & under-predicted heavier summer rain

DJF

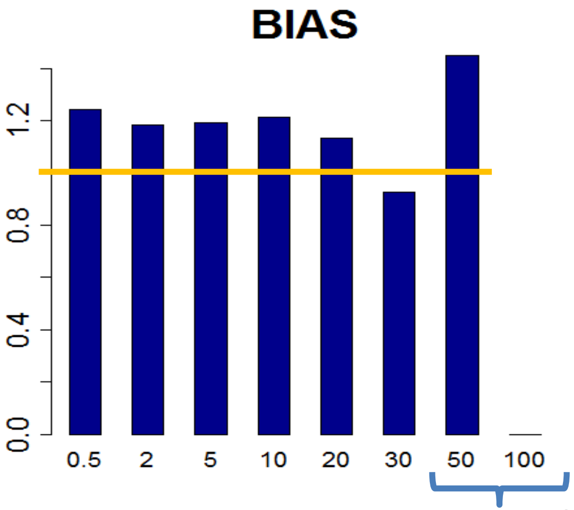

Is this meaningful?

Overall over-prediction for all precipitation ranges

Threshold = 50 mm/day			
1-day lead	OBS YES	OBS NO	Total
FCST YES	5	6	11
FCST NO	66	47462	47528
Total	71	47468	47539

Threshold = 50 mm/day			
2-day lead	OBS YES	OBS NO	Total
FCST YES	35	68	103
FCST NO	36	47400	47436
Total	71	47468	47539

Verification results (with lead times)

Equitable Threat Score

$$ETS = \frac{a - \frac{(a+b)(a+c)}{T}}{a+b+c-\frac{(a+b)(a+c)}{T}}$$

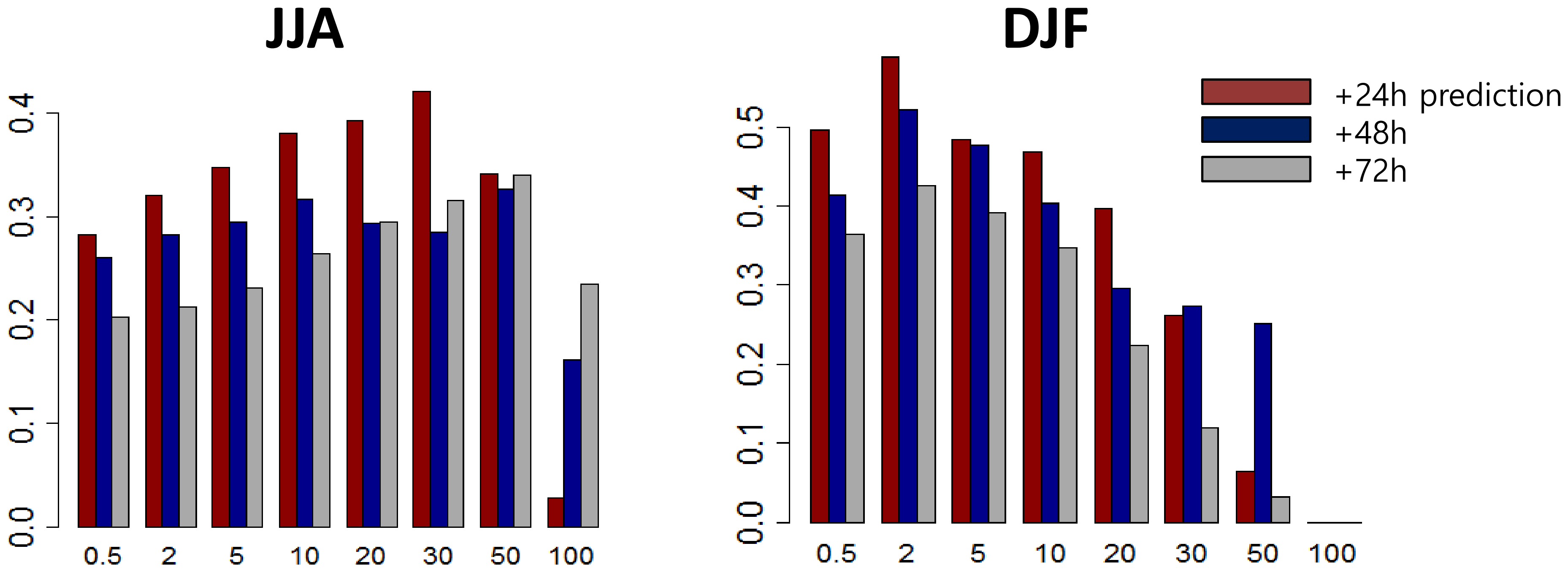

JJA

DJF

Better skill for higher thresholds in summer
Better skill for lower thresholds in winter
Prediction skill is better for winter?
Decrease of skill with forecast lead time shown in most thresholds range

Verification results (various scores)

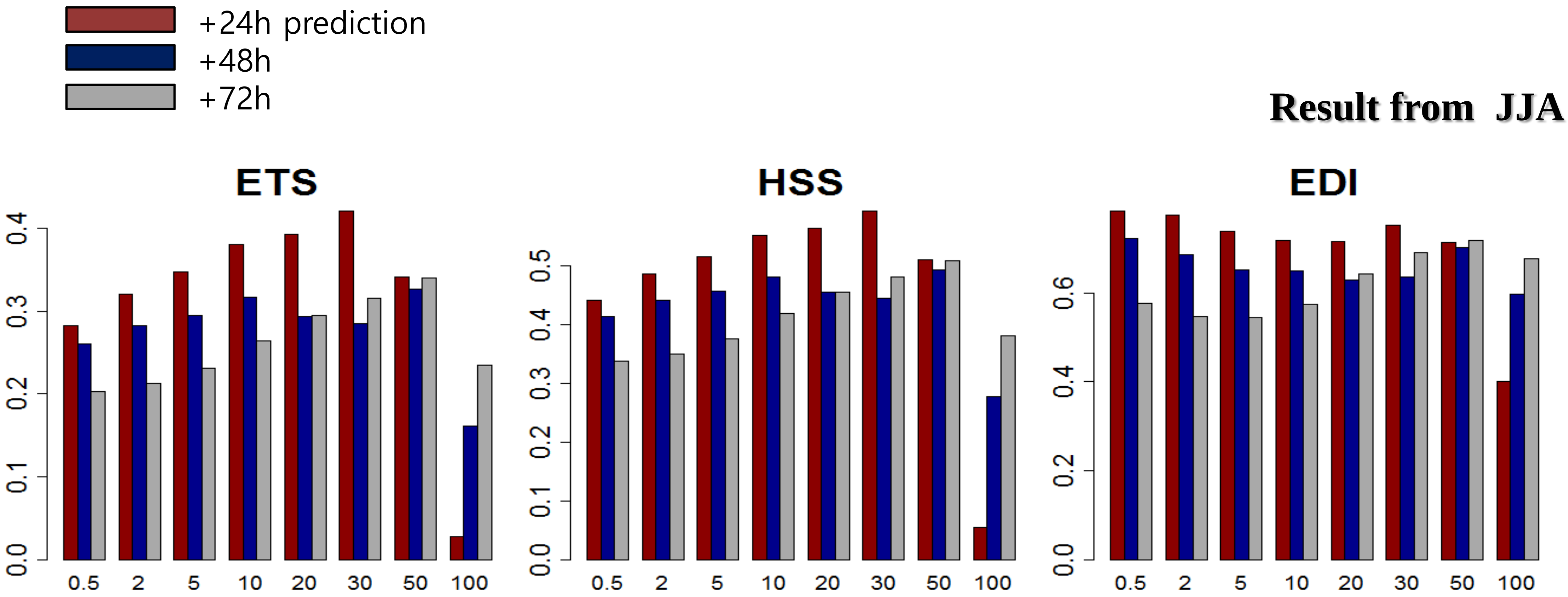

Result from JJA

$$ETS=\frac{a-\frac{(a+b)(a+c)}{T}}{a+b+c-\frac{(a+b)(a+c)}{T}}$$

$$HSS=\frac{(a+d)-\frac{(a+b)(a+c)+(c+d)(b+d)}{T}}{T-\frac{(a+b)(a+c)+(c+d)(b+d)}{T}}$$

$$\mathrm{EDI}=\frac{\log F-\log H}{\log F+\log H}$$

H = a / (a+c), hit rate

F = b / (b+d), false alarm rate

Various skill scores show different characteristics with thresholds
ETS, HSS increases with thresholds but not in EDI
Small samples size affects sharp decrease in certain skill score index like ETS, HSS

Summary

- Contingency table method is applied to verify deterministic precipitation forecasts against rain-gauge observation over Korea.
- Thresholds are selected in consideration with data distribution and extreme weather warning.

- Higher hit rate appears for light rain for both JJA and DJF.
- Higher false alarm ratio for smaller thresholds in JJA affects low skill score in summer, while higher false alarm ratio for heavier rain thresholds in DJF.
- Decrease of skill with forecast lead times is shown in most thresholds range.
- Small sample size affects certain skill scores.
- Extreme events are difficult to measure with this contingency table method.

- There are more issues about data quality control, grid-to-obs. interpolation, sample sizes, how to verify extreme events.

Verification results with lead times, DJF

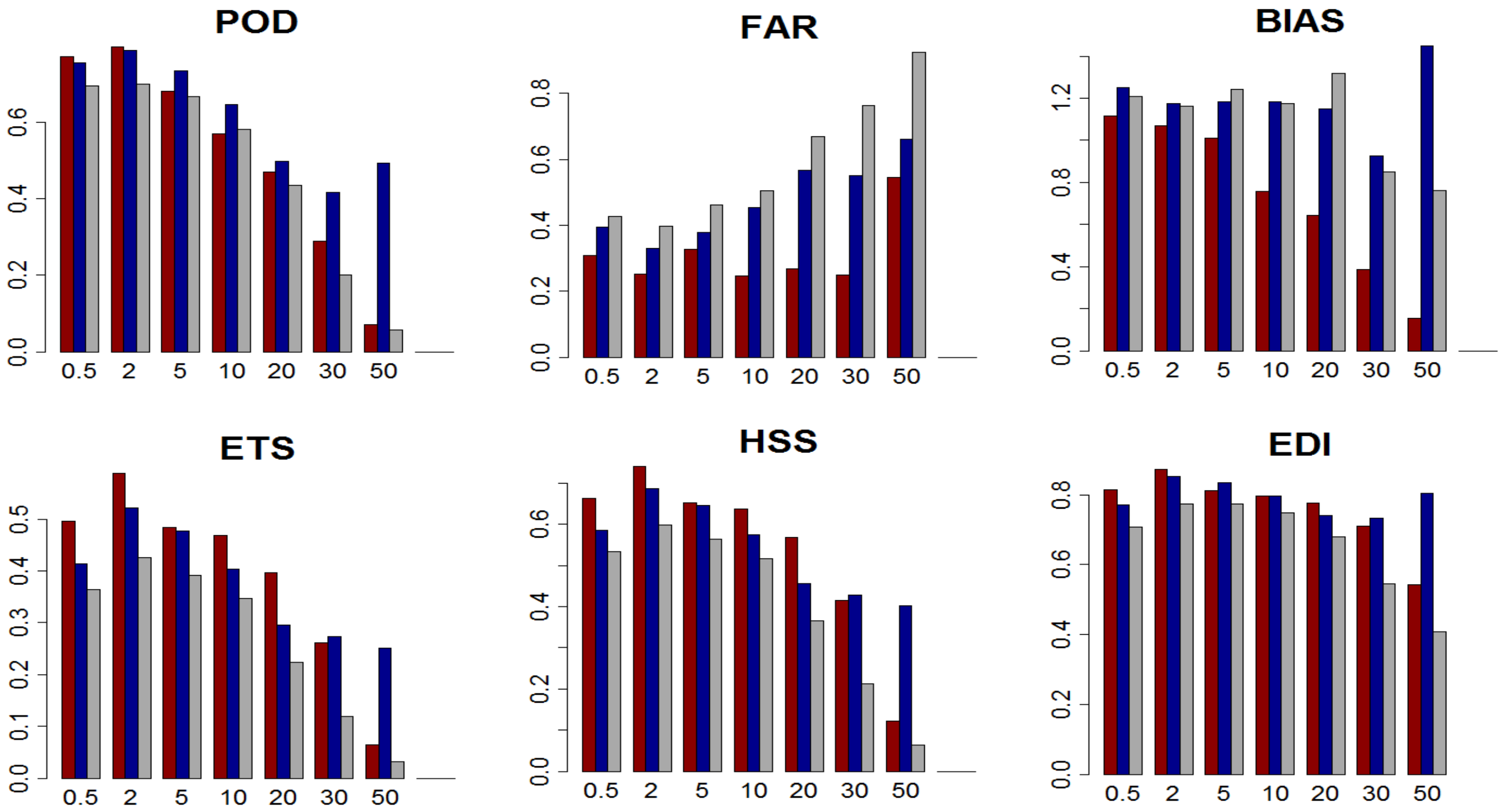

As forecast lead time is longer,
POD decreasing False alarm increasing, BIAS increasing…
Skills decreasing

till sample number issues…

threshold = 100 mm/day			
	OBS YES	OBS NO	Total
FCST YES	11	13	24
FCST NO	366	49353	49719
Total	377	49366	49743

Threshold = 50 mm/day			
	OBS YES	OBS NO	Total
FCST YES	573	269	842
FCST NO	789	48112	48901
Total	1362	48381	49743

Threshold = 30 mm/day			
	OBS YES	OBS NO	Total
FCST YES	1295	447	1742
FCST NO	1209	46792	48001
Total	2504	47239	49743

JJA16

threshold = 100 mm/day			
	OBS YES	OBS NO	Total
FCST YES	0	0	0
FCST NO	9	47530	47539
Total	9	47530	47539

Threshold = 50 mm/day			
	OBS YES	OBS NO	Total
FCST YES	5	6	11
FCST NO	66	47462	47528
Total	71	47468	47539

Threshold = 30 mm/day			
	OBS YES	OBS NO	Total
FCST YES	93	31	124
FCST NO	229	47186	47415
Total	322	47217	47539

DJF15/16